Aus dem

Institut für Kardiovaskuläre Physiologie und Pathophysiologie im Walter-Brendel-Zentrum für Experimentelle Medizin

Ludwig-Maximilians-Universität München

Renal CD64+ MPs protect kidney in both cisplatin and ischemia reperfusion induced acute kidney injury

Dissertation
zum Erwerb des Doctor of Philosophy (Ph.D.)
an der Medizinischen Fakultät der
Ludwig-Maximilians-Universität München

vorgelegt von
Xingqi Ji

aus
Zhenjiang

Jahr
2023

Mit Genehmigung der Medizinischen Fakultät der
Ludwig-Maximilians-Universität München

Erstes Gutachten:	Prof. Dr. Barbara Schraml-Schotta
Zweites Gutachten:	Prof. Dr. Hans-Joachim Anders
Drittes Gutachten:	Prof. Dr. Maciej Lech
Viertes Gutachten:	Prof. Dr. Volker Vielhauer

Dekan:	Prof. Dr. med. Thomas Gudermann

Tag der mündlichen Prüfung: 26.10.2023

Table of Contents

Abstract *7*

1 Introduction *10*

1.1 Mononuclear phagocytes (MPs) system contains diverse subsets with overlapping markers **10**

1.2 Dendritic cells are CDP derived professional antigen presenting cells **10**

1.3 Macrophages derived from multiple progenitors majoring in phagocytosis **11**

1.4 Kidney contains diverse MP subsets **13**

1.4.1 Renal cDC1 quantity is low 13

1.4.2 Markers for cDC2 identification in kidney overlap with macrophage markers 14

1.4.3 Renal CD64+ MPs exist in kidney with large quantity revealed by lineage tracing model 14

1.5 MP depletion models reveal complex functions of renal MPs in AKI **15**

1.5.1 CD11c-DTR model depletes all MPs with Clec9a expression history 15

1.5.2 CD11b-DTR model targets cDC2 and macrophage 16

1.5.3 Clodronate liposomes removes all renal MPs 16

1.5.4 Clec9acreCD64iDTR model depletes renal CD64+ MPs efficiently and specifically 17

2 Aims of study *17*

2.1 To study MPs function in AKI **17**

2.2 To investigate mechanism of how MPs mediate immune responses in AKI **18**

3 Materials and methods *18*

3.1 Animal husbandry **18**

3.2 Genotyping **18**

3.3 Cell isolation **20**

3.4 Flow cytometry **22**

3.5 DT treatment **23**

3.6 Cisplatin induced AKI **23**

3.7 Injury score **23**

3.8 Immunofluorescence microscopy **25**

3.9 Tissue paraffin embedding, section and hematoxylin and eosin staining 26

3.10 Cytokine qPCR detection 26

3.11 Ischemia reperfusion induced AKI 28

3.12 Glomerular filtration rate (GFR) detection 28

3.13 Cell sorting 29

3.14 In vitro MP histone stimulation 29

3.15 Cytokine Legendplex detection 29

3.16 Statistical analysis 30

3.17 Antibody list 30

4 Results 32

4.1 MPs with Clec9a expressing history play important role in cisplatin induced AKI 32

4.1.1 BUN and creatinine increased in Clec9acreRosaYFP mice after 48 hours cisplatin treatment 32

4.1.2 cDC1 and cDC2 are lost from inflamed kidney 33

4.2 Depletion of MPs with Clec9a expressing history increases kidney injury 34

4.2.1 cDC1, cDC2 and CD64+ MPs depletion increases injury severity after cisplatin treatment for 48 hours 34

4.3 cDC1 depletion in steady state is efficient and specific 37

4.3.1 cDC1 is efficiently and specifically depleted in XCR1-venus-DTR mice after DT injection for 24 hours 37

4.4 cDC2 depletion does not influence the severity of cisplatin induced AKI 39

4.4.1 cDC2 is reduced in Clec9a^{cre}IRF4$^{f/f}$ mice and other immune cell subsets do not change compare with littermate controls 39

4.4.2 BUN and creatinine do not change after cisplatin treatment for 72 hours in Clec9a^{cre}IRF4$^{f/f}$ mice 40

4.5 CD64^{+} MPs are efficiently and specifically depleted in Clec9a^{cre}CD64^{iDTR} mice in steady state 42

4.5.1 CD64^{+} MPs are depleted in kidney without affecting kidney function and architecture for 24 hours in steady state 42

4.5.2 Immune populations are not affected in spleen after renal CD64+ MPs depletion 44

4.6 CD64^{+} MPs depletion increases kidney injury severity after cisplatin treatment 46

4.6.1 CD64^{+} MPs kept depleted post cisplatin treatment for 48 hours 46

4.6.2 Injury severity is increased in CD64^{+} MPs depleted mice 48

4.6.3 Clec9a expression history is found on cDC1, cDC2, CD11b^{hi} and F4/80^{hi} cells after cisplatin treatment 49

4.6.4 Cisplatin does not induce CD64 expression on immune cell populations that normally do not express it 50

4.6.5 CD64^{+} MPs depletion in cisplatin induced AKI do not cause neutrophilia 51

4.7 CD64$^+$ MPs protect kidney function both in steady state and inflammation 53

4.7.1 GFR decreased in CD64$^+$ MP-depleted mice post IRI for 5 days 53

4.7.2 Renal cDC1, cDC2, Ly6c+, monocytes, neutrophils and T cells decreased significantly in IRI operated kidneys after CD64$^+$ MPs depletion post IRI for 5 days 55

4.7.3 CD8$^+$ T cell, Th1, Th17 and Treg decreased after CD64$^+$ MPs depletion in both contralateral and IRI operated kidneys post IRI for 5 days but not significant 56

4.7.4 cDC1 depletion in XCR1-venus-DTR mice post IRI for 3 days does not affect AKI severity 59

4.7.5 CD64+ MPs depletion 5 days after sham surgery leads to loss of kidney function 61

4.7.6 Renal B cells and T cells were decreased in CD64+ MPs depleted mice 5 days after sham surgery 63

4.7.7 CD64+ MPs depletion does not lead to neutrophilia in spleen 5 days after sham surgery 65

4.7.8 GFR does not change in CD64+ MP-depleted mice 24 hours after sham surgery 65

4.7.9 CD64$^+$ MP-depletion does not affect injury severity 24 hours after IRI surgery compare with non-depleted mice 66

4.7.10 CD64+ MPs kept depleted in contralateral kidney post IRI surgery for 24 hours 68

4.7.11 IL-6, IL-18, TNF-α and TGF-β do not change after CD64$^+$ MP-depletion 24 hours after IRI surgery 69

4.7.12 IFN-β increased significantly in culture supernatant after F4/80hi cells stimulated with histone 71

Discussion ***72***

1. Clec9a^{cre}CD64^{iDTR} mice are a powerful model to study CD64+ MPs function in cisplatin induced AKI 72

2. CD64+ MPs have an important role in maintaining normal kidney function in steady state and inflammation only 5 days after surgery 74

3. Outlook 75

References ***76***

Acknowledgements ***85***

Appendix ***86***

Publicaitons related to this work 86

Tables and Figures

Abbreviations 8
Fig. 1. Macrophages and DCs are overlapping in surface markers. 13
Table 1. List of primers for genotyping 19
Table 2. Genotyping PCR program 20
Table 3. Preparation of Percoll dilutions 22
Table 4. Scoring criteria in cisplatin induced AKI 23
Table 5. qPCR primers 27
Table 6. List of used antibodies 30
Fig. 2. Serum creatinine and BUN increased after 48 hours cisplatin treatment. 32
Fig. 3. MPs with Clec9a-expression history in cisplatin induced AKI for 48 hours. 34
Fig. 4. MPs with Clec9a-expression depletion leads to increased AKI severity. 36
Fig. 5. cDC1 is depleted efficiently and specifically in XCR1-venus-DTR mice after DT injection for 24 hours. 38
Fig. 6. cDC2 is reduced in Clec9acreIRF4f/f mice but other immune subsets do not alter. 40
Fig. 7. Clec9acreIRF4f/f mice do not show altered susceptibility to cisplatin-induced AKI. 41
Fig. 8. Clec9acreCD64iDTR mice allow for specific depletion of renal CD64+ MPs, kidney function and architecture do not change after CD64+ MPs depletion. 43
Fig. 9. No alterations of leukocyte populations in spleen from DT treated Clec9acreCD64iDTR mice. 45
Fig. 10. CD64+ MPs kept depleted in Clec9acreCD64iDTR after 24 hours DT injection and 48 hours cisplatin injection. 47
Fig. 11. CD64+ MPs depletion increased AKI severity. 49
Fig 12. Clec9a expression history of MPs post cisplatin injection for 2 days. 50
Fig. 13. Cisplatin treatment in Clec9acreRosaYFP mice do not induce CD64 expression on renal immune cell populations which usually do not express it. 51
Fig. 14. CD64+ MPs depletion does not induce neutrophilia in cisplatin induced AKI. 52
Fig. 15. CD64+ MPs depletion leads to more severe injury post IRI surgery for 5 days. 54
Fig. 16. Renal cDC1, cDC2, Ly6c+, monocytes, neutrophils and T cells decreased significantly in IRI operated kidneys after CD64+ MPs depletion post IRI for 5 days. 56
Fig. 17. CD8+ T cell, Th1, Th17 and Treg decreased but not significant after CD64+ MPs depletion post IRI for 5 days. 58
Fig. 18. cDC1 depletion does not affect kidney injury severity post IRI for 3 days. 60

Fig. 19. CD64+ MPs depletion leads to loss of kidney function in mice 5 days after sham surgery. 62
Fig. 20. Renal B cells and T cells decreased in CD64+ MPs depleted mice 5 days after sham surgery. 64
Fig. 21. CD64+ MP-depletion 5 days after sham surgery does not induce neutrophilia. 65
Fig. 22. CD64+ MP-depletion 24 hours after sham surgery does not affect GFR. 66
Fig. 23. GFR does not decrease in mice depleted of CD64+ MPs 24 hours after IRI surgery. 67
Fig. 24. CD64+ MPs kept depleted in contralateral kidney 24 hours after IRI surgery. 69
Fig. 25. IL-6, IL-18, TNF-α and TGF-β expression do not change in CD64+ MP- depleted mice 24 hours after IRI surgery. 71
Fig. 26. IFN-β increased F4/80hi cells culture supernatant after histone stimulation for 16 hours. 72

Abstract

Mononuclear phagocytes (MPs) consist of dendritic cells (DCs), macrophages and monocytes, they have important functions in mediating immune responses in tissues. It is reported in kidney contains diverse MP subsets, however, due to insufficient subset specific depletion model, the functions of these MPs are unclear in acute kidney injury (AKI). C-Type Lectin Domain Containing 9A (Clec9a) is a receptor sensing polymeric F-actin exposed in necrotic cells, and it is highly expressed on common dendritic cell progenitor (CDP) that give rise to dendritic cells (DCs), by genetic tracing of Clec9a expression histroy will specifically mark DCs but not other immune cells. In steady state the kidney contains at least 4 subsets with Clec9a expressing history, cDC1, cDC2 and a large CD64 expressing group which can be subdivided into F4/80^{hi} and CD11b^{hi} sub-populations. By using cDC1 depletion model (XCR1-venus-DTR), we found cDC1 depletion did not increase kidney injury severity after cisplatin treatment. The similar situation also happened when we depleted cDC2 in Clec9a^{cre}IRF4$^{f/f}$ mice treated with cisplatin. However, cisplatin induced injury increased significantly when we used newly generated Clec9a^{cre}CD64^{iDTR} model to deplete CD64^{+} MPs in the kidney, this result indicated CD64^{+} MPs can protect kidney in cisplatin induced AKI. By constructing ischemia reperfusion acute kidney injury, we found CD64^{+} MPs also have protective role in both steady state and inflammation state, the mechanism could be attributed to regulation of anti/pro-inflammatory cytokines produced by CD64^{+} MPs. Thus, we conclude CD64^{+} MPs protect kidney both in cisplatin induced AKI and also in ischemia reperfusion induced AKI, which may shed lights to therapeutic targeting of this population for curing AKI in the future.

Abbreviations

Abbreviation	Full name
AKI	Acute kidney injury
Arg1	Arginase 1
ATN	Acute tubular necrosis
BM	Bone marrow
BUN	Blood urea nitrogen
cDC1	Conventional type 1 dendritic cells
cDC2	Conventional type 2 dendritic cells
CDP	Conventional dendritic cell progenitor
CNS	Central nervous system
COX	Cyclooxygenase
DCs	Dendritic cells
DT	Diphtheria toxin
DTR	Diphtheria toxin receptor
E8	Embryonic day 8
E8.5	Embryonic day 8.5
E10	Embryonic day 10
E10.5	Embryonic day 10.5
E16.5	Embryonic day 16.5
EDTA	Ethylenediaminetetraacetic acid
Flt3	Fms-like tyrosine kinase 3
GFR	Glomerular filtration rate
GMPs	Granulocyte-monocyte progenitors
GM-CSF	Granulocyte macrophage colony-stimulating factor
HSC	Hematopoietic stem cell
GN	Glomerular necrosis
ITAM	Intracellular motif immunoreceptor tyrosine-based activation motif
IL1a	Interleukin 1a
IL6	Interleukin 6
IL18	Interleukin 18
IFNb	Interferon Beta
IRF4	Interferon regulatory factor 4
IRI	Ischemia reperfusion injury
KIM1	Kidney injurt marker 1
Lin	Lineage
M-CSF	Granulocyte macrophage colony-stimulating factor
M-CSFR	Granulocyte macrophage colony-stimulating factor

pDC	Plasmacytoid dendritic cells
pre-DCs	Precursors of dendritic cells
PAS	Periodic Acid-Schiff
TGFb	Transforming growth factor b
TNFa	Tumor necrotic factor a
TCR	T cell receptor
Th1	T helper cell type 1
TLR	Toll-like receptor
XCR1	X-C Motif Chemokine Receptor 1

1 Introduction

1.1 Mononuclear phagocytes (MPs) system contains diverse subsets with overlapping markers

Mononuclear phagocytes (MPs) are classified as dendritic cells (DCs), monocytes, macrophages according to their functions and phenotypes (1). However, since these MP subsets are overlapping in markers, it is difficult to distinguish their specific functions (Fig. 1). To precisely define these MPs is necessary for their function study.

1.2 Dendritic cells are CDP derived professional antigen presenting cells

Dendritic cell (DC) is a subset of immune cell that professionally presenting antigens to T cells for adaptive immune responses activation (2). DCs are conventional dendritic cell progenitor (CDP) derived cells which are generated from bone marrow (3). CDP is characterized by Lin^-, $CD115^+$, $Flt3^+$ and $M\text{-}CSFR^+$ (4). When CDP is stimulated by Flt3 ligand, it can differentiate into pre-DCs marked by CD11c and Siglec-H, and pre-DCs will successively give rise to $CD11c^+MHCII^+$ cell populations which are defined as DCs (5).

As professional antigen presenting cells, DCs can uptake and process antigen with high efficiency. After capturing and digesting endogenous or exogenous pathogens, MHC receptor will present the antigen on dendritic cell´s surface, once antigen-MHC complex is recognized by TCR and co-stimulatory molecules CD28 expressed on T cells, T cell mediated adaptive immune response is activated to eliminate pathogens (6).

DCs can present both endogenous and exogenous antigens to T cells, and the mechanisms of each pathway are different. For exogenous antigen presentation, such as antigens from bacteria, DCs capture these antigens by Fc receptor and internalize them by phagocytosis. After phagocytosis these antigens are digested into small amino acid fragments in acidic lysosomes. Endogenous antigen presentation is mediated by MHCI which expressed on all nucleated cells. Since DCs have large quantity of diubiquitin, it makes cytosolic proteins easily recognized and degraded by proteasomes and presented on MHCI for T cell receptor binding (7-9).

cDCs according to phenotypes can be classified as cDC1, cDC2 and pDC. cDC1 is characterized by surface markers MHCII, CD11c, CD103, CD24, Clec9a and XCR1, it can also be distinguished by transcription factors such as IRF8, Batf3 and ID2 (2, 10, 11). Functionally, cDC1 is specialized in cross-presentation, it is a process that cDC1 presents extracellular antigens to $CD8^+$ T cells via MHCI (12). cDC2 is highly expressing CD11b and SIRPa beside MHCII and CD11c, it is also marked by transcription factor IRF4 (2). The major function of cDC2 is to activate $CD4^+$ T cells by MHCII mediated antigen presentation (2, 8). pDC is expressing B220, $Ly6C^+$ and Siglec-H, it can produce type I interferons which have anti-viral function and also mediate maturation of B cells (13, 14).

Another important function of DCs is to secret diverse cytokines to mediate immune responses. IL-1 is a pro-inflammatory cytokine involved in pathogenesis of numerous diseases. It activates the acute phase immune responses such as matrix metalloproteinases production, chemokine production and other leukocytes maturation (15-17). It is reported DCs can produce IL-1b during LPS stimulation, which may indicate the therapeutic benefits of treating endotoxemia patients with IL-1b antagonist (18-20). IL-6 is another pro-inflammatory cytokine produced by dendritic cells, it is essential for T helper 2 cell and T helper 17 cell differentiation, and full knock out of IL-6 in HDM-induced asthma in mice ameliorates eosinophilia in lungs (21-24). Beside pro-inflammatory cytokines, DCs can also produce anti-inflammatory cytokine such as IL-10. IL-10 is a key cytokine to regulate to control T cell mediated immune responses to pathogens for preventing chronic inflammation and tissue damage (25-28).

1.3 Macrophages derived from multiple progenitors majoring in phagocytosis

Macrophage is an important component in innate immune system. They reside in various tissues and function as microorganism and tissue damage scavenger. Macrophages can be divided into embryonic yolk sac (YS) precursor derived macrophage and definitive hematopoietic stem cell (HSC) derived macrophage. YS derived macrophages firstly appear in blood island on embryonic day 8 (E8), and then migrate into different organs from

E8.5 to E10 and start to proliferate in these organs. HSCs appear in fetal liver on E10.5 and successively give rise to HSC derived macrophage in adult tissues (29-32).

Phagocytosis is the most prominent function of macrophages. By phagocytosis, macrophage can capture and remove pathogens and apoptotic cells to protect tissues. This process is mediated by scavenger receptors (FcγRs). During phagocytosis, FcγRs firstly bind with IgG-pathogen complex, and then FcγR intracellular motif immunoreceptor tyrosine-based activation motif (ITAM) initiates downstream signaling pathways to form pseudopods to internalize and digest pathogens (33, 34).

Macrophages can also produce cytokines to mediate immune responses. Tumor necrosis factor (TNF-a) as a glycoprotein to induce necrosis in tumors is one of the major cytokines produced by macrophage when it meets microenvironmental stimuli. For instance, hypoxia signaling via HIF-1a activates macrophage to produce TNF-a in COX dependent pathway. Similar to TNF-a, IL-1 is another pro-inflammatory cytokine produced by macrophage at the early stage of inflammation, it can promote the synthesis of acute phase protein in liver and stimulates central nervous system to induce prostaglandin production (35-37). Macrophages can also sense IL-1 secreted by apoptotic cells and scavenge them (15, 38). Macrophage can produce IL-6 to promote B cell differentiation and cytotoxic T cell activation (39, 40). It is reported IL-6 produced by macrophage inhibits neuroinflammation in vivo which may indicate IL-6´ s anti-inflammatory function in CNS and a broader investigation about macrophage´s polarization in brain (38, 40).

The conventional markers used to identify macrophages includes F4/80, CD11b, CD64, MerTK, CSF1-R, CD68 and MHCII (41-44). However, since some of the markers such as CD11b, F4/80, CD68 and MHCII are also expressed by DCs according to recent publications, it is hard to distinguish them just by these markers (Fig. 1) (45-47). In order to investigate macrophage and DCs function in specific organs both in steady state and inflammation, new strategy should be developed.

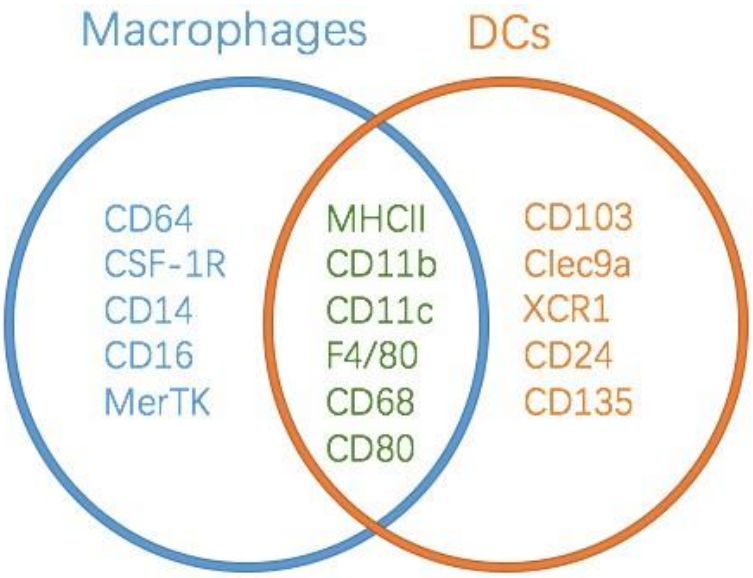

Fig. 1. Macrophages and DCs are overlapping in surface markers. Macrophages (blue circle) and DCs (orange circle) are both highly expressing MHCII, CD11b, CD11c, F4/80, CD68 and CD80 (green labeled markers), it is difficult to distinguish this two MP subsets by using these overlapping markers.

1.4 Kidney contains diverse MP subsets

In non-inflammatory steady state, the adult kidney contains diverse MP subsets such as macrophages and DCs, DCs can be distinguished from macrophages by their Clec9a expressing history. Salei et al. reported the kidney contains at least 4 subsets of MPs with Clec9a expression history, and during inflammation some MP subset undergoes phenotypic reprogramming, which increases the diversity and also the difficulty to distinguish them from each other (48, 49).

1.4.1 Renal cDC1 quantity is low

In steady state, cDC1 takes up to 2% of all immune cells in kidney (48). Although cDC1 frequency is low in kidney, it is reported renal cDC1 deteriorates injury severity in acute tubular necrosis (ATN) (50, 51). Beside ATN, cDC1 also has important function in ischemia reperfusion induced acute kidney injury. Li et al. reported cDC1 depletion by

Clec9a^{cre}IRF8$^{f/f}$ leads to increased severity post ischemia reperfusion injury, it is possibly by mediating inflammatory cytokine production derived from Th1 cells and cytotoxic CD8^{+} T cell (51).

1.4.2 Markers for cDC2 identification in kidney overlap with macrophage markers

Renal cDC2 express MHCII, CD11c, CD11b, Clec4a and CX3CR1 , however, some markers are also expressed by macrophages such as MHCII and CD11b, which makes it difficult to distinguish these 2 populations in kidney (2, 52, 53). Identification of cDC2 and macrophage according to specific transcription factor makes some progress on this problem. Considering cDC2 is dependent on Flt3L, and macrophages do not need Flt3L to proliferate, by using Flt3L knock out mice researchers can identify macrophage location in the kidney (54-58). Guilliams et al. reported a method to define DCs and macrophage according to surface markers combined with ontogeny and transcription factor, according to this method they defined cDC2 as CD11c^{hi}CD26^{hi}IRF8^{low}IRF4^{hi}, macrophage as CD11c^{low}CD26^{low}IRF4^{int}IRF8^{int}, however, cDC2 and macrophage may undergo transcriptional reprogramming in inflammation which leads to difficult distinguish of these 2 populations (1). Liu et al. reported Ms4a3 is specifically expressed on granulocyte-monocyte progenitors (GMPs) but not CDP, so that macrophage derived from monocyte will be labeled but not DCs, by using this model renal cDC2 and macrophage can be distinguished, however, it is reported macrophages and DCs may undergo reprogramming during development or inflammation, it is possible that CDP may express Ms4a3 during development transiently that leads to the labeling of cDCs which will mix with monocyte derived macrophage (59).

1.4.3 Renal CD64+ MPs exist in kidney with large quantity revealed by lineage tracing model

Clec9a is specifcally expressed on CDP, by constructing Cre recombinase down stream of Clec9a promotor with floxed stop codon YFP under Rosa promotor, all of CDP derived cells will be labeled with YFP (11). By using this model, Schraml et al. reported kidney contains one large MP population with Clec9a expressing history with MHCII, CD11c,

F4/80 and CD64 expression. This population also reported by other groups, Yang et al. indicated this population ($CD45^+F4/80^+CD11b^+$) can exacerbate tubule injury in IRI model, and recruitment of this population is CCR2-dependent (60). Berry et al. showed disruption of CCL2-CCR2 axis can cause abnormal chemokine production of this population ($F4/80^{hi}$) in kidney (61). Lever et al. showed CD64+$F4/80^{hi}$ population in kidney downregulated MHCII in IRI (49). Stamatiades et al showed kidney resident macrophage ($F4/80^{hi}$) checks the protein transportation and small particles with molecule weight between 20 to 700 kDa in the kidney interstitium (62). In conclusion, these $F4/80^{hi}$ cells ($CD64^+$ MPs) are taking large part in kidney, to decipher their function in kidney is important to develop therapeutic method to treat acute and chronic kidney diseases.

1.5 MP depletion models reveal complex functions of renal MPs in AKI

In order to study different MPs function in acute kidney injury, many deletion models that targeting these populations are developed. However, since renal macrophages and DCs are overlapping in many surface markers such as CD11b and CD11c (Fig. 1), so that diphtheria toxin (DT) mediated depletion models like CD11b-DTR or CD11c-DTR will not be limited to cDCs depletion but also targeting macrophages, in order to study MP subset's function respectively, specific depletion model needs to be built up.

1.5.1 CD11c-DTR model depletes all MPs with Clec9a expression history

cDCs are immune cells that professionally present antigens to activate T cell mediated immune responses, their role in kidney diseases is important. Since CD11c is conventional DC marker for all MPs with Clec9a expression history (63), to construct diphtheria toxin receptor (DTR) under CD11c promotor allowing both cDC1, cDC2, $CD11b^{hi}$ and $F4/80^{hi}$ depletion. For assessing cDCs´ function in AKI, Lu et al. reported by using CD11c-DTR model, ischemia reperfusion induced AKI severity did not have significant change after cDCs depletion, indicating cDCs´ role in ischemia reperfusion induced AKI is negligible (64). On the contrary, Tadagavadi et al. reported cDC depletion in cisplatin induced AKI protects kidney in CD11c-DTRtg mice (65). The inconsistency between these 2 studies could be attributed to different reasons, one is the order to construct injury and depletion.

In the first study, cisplatin induced AKI is carried out after DC depletion, and in the second study the IRI is constructed before DC depletion, it may lead to different results. Secondly, the mechanism of cisplatin induced AKI is different from the IRI AKI model. Ischemia/reperfusion injury (IRI) is induced by short and temporary damage of the blood flow to the particular organ (66-68). IRI can induce a strong inflammation and oxidative stress to the organ which damage the organ function, however, cisplatin can combine with DNA and cause kidney tubular necrosis and apoptosis (69, 70), it may make the result different from IRI. In conclusion, cDCs´ function in AKI still needs more investigation.

1.5.2 CD11b-DTR model targets cDC2 and macrophage

CD11b-DTR is designed for $CD11b^+$ cell depletion, since macrophage, monocyte, neutrophil and recently defined $CD64^+$ MPs are all highly expressing CD11b, all of them will be depleted. Lu et al. reported CD11b-DTR mediated depletion do not change IRI severity, it is possibly they depleted not just cDC2 but also other populations with CD11b expression (64). However, contradictory results reported by Li et al. claiming that tubular injury deteriorated after $CD11b^+$ macrophage depletion in CD11b-DTR mice post IRI, indicating macrophages have protective role in IRI (71). In fact, both of the studies did not take into consideration of the heterogeneity of $CD11b^+$ immune populations in kidney, and by using CD11b-DTR model to investigate either cDC2 or macrophage in kidney may not be a perfect choice.

1.5.3 Clodronate liposomes removes all renal MPs

Clodronate liposomes can be uptaken by MPs and induce apoptosis. Ferenbach et al. reported clodronate liposomes administration in IRI AKI model demonstrated macrophages´ exacerbating role in AKI (72). However, since all of MPs will capture clodronate liposomes and lead to elimination, the protective role cannot be specifically attributed to loss of macrophage but could also come from the loss of other MP populations. Kitamoto et al. reported in ureteral obstruction induced AKI, clodronate liposomes can selectively deplete $F4/80^+$ DCs and macrophages, but according to their data, T cells,

$CD11b^+$ cells and $CD11c^+$ cells are also depleted when mice are injected with clodronate liposomes in steady state, indicating the clodronate liposomes mediated depletion may not be specific (73).

1.5.4 Clec9acreCD64iDTR model depletes renal CD64+ MPs efficiently and specifically

Schraml et al. reported renal $CD64^+$ MPs are labeled with YFP in $Clec9a^{cre}Rosa^{YFP}$ mice, for build-up of this model, they constructed Cre recombinase under control of Clec9a promoter and cross with mice inserted of floxed stop codon YFP under Rosa26 promoter, the descendants will be labeled with YFP signal only in cells with Clec9a expressing history. Their results indicate renal $CD64^+$ MPs have Clec9a expressing history (63, 74). Since renal cDC1 and cDC2 can be distinguished from $CD64^+$ MPs by CD64 expression, Pakalniskyte et al. constructed floxed stop codon under control of CD64 promotor and crossed it with $Clec9a^{cre}$ mice, so in $Clec9a^{cre}CD64^{iDTR}$ mice the $CD64^+$ MPs can be specifically depleted without affecting cDC1 and cDC2. Beside cDCs, other immune subsets such as B cell, T cell, neutrophil, and monocytes are not affected after $CD64^+$ MPs depletion. This model shows $CD64^+$ MPs depletion efficiency, specificity and potential for studying this population´s function both in steady state and inflammation (75).

2 Aims of study

2.1 To study MPs function in AKI

In order to decipher each MP´s function in AKI, we will use different depletion mice models to target each MPs respectively, and then induce kidney injury on these mice to check injury severity. The streamline of reaching this aim is described below.

- Depletion of total renal MPs with Clec9a expressing history to determine their function in AKI
- Depletion of each subset with Clec9a expressing history to determine its function in AKI

2.2 To investigate mechanism of how MPs mediate immune responses in AKI

In order to investigate mechanism of how MPs mediate immune responses in AKI, try to target specific genes that up/down regulated in both tissue level and cell level. The streamline of reaching this aim is described below.

- In both cisplatin and IRI induced AKI model, we will check pro-inflammatory and anti-inflammatory markers by using qPCR.
- In order to check renal MPs´ cytokine production, we will sort MPs and stimulate them with histone to check cytokine production.

3 Materials and methods

3.1 Animal husbandry

Clec9a$^{tm2.1(icre)Crs}$(Clec9a^{cre}) (74), Gt(ROSA)26Sor$^{tm1(EYFP)}$Cos(Rosa26^{YFP}) (76), Gt(ROSA)26Sor$^{tm1(HBEGF)Awai}$ (Rosa26^{iDTR}) (77), IRF4-flox (78), XCR1-venus-DTR (79), CD64-lox-STOP-lox-DTR and C57BL/6JRccHsd mice bred and fed in the University of Munich at BMC, the condition for mice breeding is specific pathogenfree, with a 12 hours light and 12 hours dark cycle. Mice used in this research are between 8-14 weeks. All animal related operations/procedures were performed under both institutional and national regulations/guidelines for animal welfare and approved by the Government of Upper Bavaria.

3.2 Genotyping

Ear snips were collected for genotyping by animal caretakers from animal facility in University of Munich at BMC. Ear snips were transferred into 1.5ml EP tube containing 300 µl quick lysis buffer consist of 150 mM NaCl, 10 mM Tris, 5 mM EDTA, 0.05 % 0.2 mg/ml Proteinase K, NP-40. Ear snips were put and digested in the thermoshaker (Eppendorf) at 56 °C with 300 rpm for 3 hours, after digestion they were inactivated by increasing temperature to 90 °C and shaked with 300 rpm last for 10 min. After inactivation

centrifuge with 13000 g for 5min and collect the supernatant. 1 µL supernatant was taken for genotyping.

Table 1. List of primers for genotyping

Genotyping primers	5´-3´
Clec9a-Cre-BS49 Common	AAA AGT TCC ACT TTC TGG ATG ATG A
Clec9a-Cre-BS47 Wild type	GGC TCT CTC CCC AGC ATC CAC A
Clec9a-Cre-A65 Mutant	TCA CTT ACT CCT CCA TGC TGA CG
Rosa26-YFP2 -1 Sense fwd	AAA GTC GCT CTG AGT TGT TAT
Rosa26-YFP2 -2 mut rev	GCG AAG AGT TTG TCC TCA ACC
Rosa26-YFP2 -3 wt rev	GGA GCG GGA GAA ATG GAT ATG
Rosa 1	AAA GTC GCT CTG AGT TGT TAT
Rosa 3 H 878	GGA GCG GGA GAA ATG GAT ATG
iDTR-R BBO 0164 H033	AAT AGG AAC TTC GTC GAG C
20418 _Irf4g/wt H185	TGG GCA CCT CTA CTG TCT GG
20419_ Irf4wtR_EV H187	CTC TGG GGA CAT CAG TCC T
20420_IrftgREV H187	CGA CCT GCA GCC AAT AAG C
XCR1-a (AKM 258)	CTA TCT TAA GAT TTC TCA GGG CCA GTC TAC
XCR1-b (AKM 259)	CAG GAC AAT GGT AGA GAT GGT GGA AAA G

XCR1-c (AKM 260)	CTG CAG CCA GAA AGA GCT TCA G
CD64.3 H688	TCA GGG TCA ACT TTG GGA AG
CD64.4 H671	CCA AAT GTA ACT TGG CTG GGT C
CD64.5 H671 47-5293- 3/3	GGT ACT CTG TTC TCA CCC TTC

Table 2. Genotyping PCR program

Locus	Annealing temperature (°C)	Extension time (s)	Expected results
Clec9a-Cre	60	40	WT: 407 bp
			Mut: 597 bp
Rosa26-YFP	60	60	WT: 320 bp Mut: 600 bp
Rosa26iDTR	61	60	WT: 600 bp Mut: 845 bp
Irf4-flox	65 (-0.5 per cycle)	15	WT: 142 bp Mut: 91 bp
XCR1-Venus-DTR	62	30	WT: 450 bp Mut: 450 bp
Cd64-lox-STOPlox-DTR	60	30	WT: 407 bp Mut: 561 bp

3.3 Cell isolation

- Splenocyte isolation

Spleens were firstly isolated from mice and then transferred into 5ml bijoux vial which containing 0.5 ml RPMI, cut spleen into tiny pieces (the smaller the better). Prepare a 2x master mix of Collagenase IV and DNAse I. Add 0.5 ml of the 2x master mix to bijoux vial containing the spleen to reach a working concentration with 200U/ml collagenase IV and

0.2 mg/ml DNAse I (the total volume in bijoux vial is 1 ml), and then incubate in a shaking incubator with 150 rpm for 30 min at 37°C. After incubation pipette digested tissue several times in order to break tissue into smaller pieces and then pass the tissue through the 70 µm strainer into 50 ml Falcon tube. Wash strainer with cold FACS buffer (PBS+1% FCS+2.5 mM EDTA+0.02% Sodium Azide). Add 30 ml cold FACS buffer into 50 ml Falcon tube and centrifuge with 1350 rpm for 5 min at 4°C. Discard the supernatant and loosen cells with Eppendorf rack. Re-suspend cells with 2 ml red blood cell lysis buffer (Red Blood Cell Lysing Buffer Hybri-Max, Sigma Aldrich), lyse cells for 2 min at room temperature. Top up Falcon tube with cold FACS buffer to stop the digestion reaction and then centrifuge for 5 min with 1350 rpm at 4°C. Discard supernatant and re-suspend cells in 2.5 ml FACS buffer. Pass cells through strainer, count live cells for further use.

- Kidney immune cell isolation

Kidneys were perfused with cold PBS before isolation, then kidneys were isolated from mice and then transferred into 5ml bijoux vial which containing 1 ml RPMI, cut kidneys into tiny pieces (the smaller the better). Prepare a 2x master mix of Collagenase IV and DNAse I. Add 1 ml of the 2x master mix to bijoux vial containing the kidneys to reach a working concentration with 200 U/ml collagenase IV and 0.2 mg/ml DNAse I (the total volume in bijoux vial is 2 ml), and then incubate in a shaking incubator with 150 rpm for 1 h at 37°C. After incubation pipette digested tissue several times in order to break tissue into smaller pieces and then pass the tissue through the 70 µm strainer into 50 ml Falcon tube. Wash strainer with cold FACS buffer (PBS+1% FCS+2.5 mM EDTA+0.02% Sodium Azide). Add 30 ml cold FACS buffer into 50 ml Falcon tube and centrifuge with 1350 rpm for 5 min at 4°C. Discard the supernatant and loosen cells with Eppendorf rack. Re-suspend kidney cells with 4 ml 70% percoll into 15 ml Falcon tube, then overlay 37% percoll on the top with pipette boy slowly, after that overlay 30% percoll on the top with pipette boy slowly. Centrifuge with 2,000 rpm for 30 min at room temperature (ACC:3, DEC:3). After centrifugation, use vacuum pipette to discard the top 30% percoll layer, then use pipette to carefully collect the intermediate leukocyte layer between 70% percoll and 37% percoll into another 15 ml Falcon tube. Top up Falcon tube with 15 ml FACS buffer and centrifuge with

1350 rpm at 4°C for 5 min and discard supernatant. Collect the pellet for further use. Percoll dilutions were prepared according to Table 3.

Table 3. Preparation of Percoll dilutions

Dilution (%)	Isotonic Percoll (ml)	Additive (ml)
70	28	12
37	14.8	25.2
30	6	14

3.4 Flow cytometry

Transfer the required amount of cells into a 96 well V-bottom plate. Centrifuge at 400 g for 3 min at 4°C. Discard supernatant by quickly inverting the plate over a waste container and then tap the plate onto a paper towel to collect the last drops of liquid (for this step it is critical to hold the plate upside down until dipping onto paper to avoid cell loss). Resuspend cells in 25 µl FACS buffer. (Cells can be stored at 4°C or on ice until the Fc-Block and staining mix are prepared). Prepare a 2x master mix of Fc-block reagent by multiplying the number of samples (plus one or two extra well) by 25 µl. Then add the required amount of Fc-block (to avoid unspecific binding of staining antibodies to Fc-gamma receptors). Add 25 µ 2x Fc-block mix and incubate for 10 minutes at 4°C (or on ice). TIP: This incubation step can be extended (for instance if preparation of the staining master mix takes longer). Prepare 50 µl of 2x antibody staining mix per sample in a 1.5 ml Eppendorf tube, then add 50 µl 2x antibody staining mix to each sample and incubate for 30 minutes at 4°C. Add 100 µl of FACS buffer per sample. Centrifuge at 400 g for 3 min at 4°C. Discard supernatant by quickly inverting the plate over a waste container and then dipping the plate onto a paper towel to collect the last drops of liquid. Resuspend cells in 200 µl of FACS buffer. Centrifuge at 400 g for 3 min at 4°C and discard supernatant again. Resuspend cells in 100uL and store in the dark until acquisition. Flow cytometry analysis was performed with LSR Fortessa (BD Biosciences), FlowJo v.10 software (FlowJo LLC) was used for data acquisition analysis. Cell quantification was performed by using CountBright™ Absolute Counting Beads (Thermo Fisher Scientific).

3.5 DT treatment

Target mononuclear phagocytes were depleted in 8-14-week-old Clec9a^{cre}CD64^{iDTR}, Clec9a^{cre}Rosa^{iDTR} and XCR1-venus-DTR mice by diphtheria toxin i.p. injection of 25 ng/g of body weight. Control mice were injected with DT/PBS according to their genotype. 24 h after DT/PBS injection mice were either analyzed for immune cell dynamics or subsequently injected with cisplatin to induce acute kidney injury.

3.6 Cisplatin induced AKI

Acute kidney injury was induced in adult male or female Clec9a^{cre}CD64^{iDTR}, Clec9a^{cre}Rosa^{iDTR}, Clec9a^{cre}IRF4$^{f/f}$, XCR1-venus-DTR and C57B/6JRccHsd mice by i.p. injection of 15 mg/kg (female) or 25 mg/kg (male) body weight cisplatin. Baseline mice were injected with an equal amount of NaCl. Organs and blood were collected 4872 hours after cisplatin injection or sacrificed if mice meet termination criteria according to acute injury score sheet. Blood serum was collected for serum creatinine and blood urea nitrogen (BUN) measurement animal hospital at Munich (Tierklinikum München).

3.7 Injury score

The animals are monitored twice a day for up to 24 hours after the cisplatin injection. Then that happens scoring 2 times daily so that the condition of the animals is monitored both from 8-10 am and 4-6 pm. By doing this is to be able to intervene immediately if the termination criteria are met. Reaching 5-10 points is classified as low stress, it will be no further action taken. Achieving a total of 15-20 points is considered a mean stress and the animal continued in the experiment. If there is no improvement, that applies achievement of a score of 15-20 points over a period of 48 hours as a termination criterion, and the animals are killed painlessly. If a total of 25 points is reached, the experiment is terminated immediately and the affected animal is killed immediately and painlessly.

Table 4. Scoring criteria in cisplatin induced AKI

1. behavior	score

Attentive, active behavior such as nest building, climbing	0
Reduced alertness, response to external stimuli	5
Apathetic, no response to external stimuli, self-isolation	25

2. Maintenance condition	score
Fur: smooth, shiny, body orifices clean	0
Decreased or excessive grooming	5
Fur: dull, shaggy	15
Fur: erect, glued; Body orifices: dirty	15

3. Breathing	score
Physiologically inconspicuous breathing, calm, even	0
Forced or gasp breathing	25

4. Posture	score
physiological	0
Back arched, crouching posture	15

5. Body weight reduction as a percentage of the initial weight	score
0-5% loss, increase	0
Loss 6-10%	5
Loss 11-15%	10
Loss 16-19%	20
Loss = 20% or more	25

3.8 Immunofluorescence microscopy

Kidneys were fixed with 1% paraformaldehyde at 4 °C overnight, on next day kidneys were transferred into 30% sucrose at 4 °C overnight. On next day the kidneys were transferred to Tissue-Tek O.C.T. (Sakura), then immediately freeze on dry ice for 10 min and stored in -80°C. During kidney section process, set the thickness of each slice with 10 µm by using Leica CM3050S cryostat, section step must be performed at -20 °C. During staining process, firstly thaw the sections to dry and then rehydrated in PBS, after thawing sections permeabilizing the sections with cold Acetone. Take sections from acetone, wipe off acetone left-over and circle the kidney tissue on the glass with a PAP Pen (Kisker Biotech GmbH), then use 10 % goat serum in PBS to block the kidney tissue on glass for 1 h at room temperature. Make sure the surrounding of the tissue is humidified. During blocking, prepare the staining master mix by diluting antibody with blocking buffer. After blocking is finished, wipe off the blocking buffer and drop the antibody master mix on the tissue and incubate for 2 h at room temperature, make sure the surrounding is humidified. After staining, wipe off the master mix in the circle and then wash the sections with PBS twice, then use ProLong™ Diamond Antifade Mountant (Thermo Fisher Scientific) to mount the section with glass, stored in dark chamber overnight at room temperature and kept at 4°C before imaging. Microscopy imaging was performed in University of Munich at the Core Facility Bioimaging of the Biomedical Center by using Leica SP8X WLL microscope, it is equipped with 405nm laser and WLL2 laser (470 - 670nm). Imaging of target cells in this research is by using fluorophores below: AF594 (excitation 592nm, emission 605-640nm), AF647 (excitation 646nm, emission 656-718nm), BV421 (excitation 405nm, emission 415470nm) and AF555 (excitation 553nm, emission 563-591nm). Imaging of pictures were recorded by using sequential imaging. All fluorophores were detected and imaged by using hybrid detector. All pictures were saved and imported into Fiji for adjustment and adding scale bars. For quantification of $CD64^{+}$ MPs in tissue sections 6 squares were chosen randomly from both renal cortex and medulla among all tile-scans for quantification.

3.9 Tissue paraffin embedding, section and hematoxylin and eosin staining

Firstly, fix kidneys with 4% formalin diluted by PBS for 24 h. Then put kidneys into 70% ethanol and change 2 times, 1 hour for each change, then kidneys go into 80% ethanol for 1 h, and then put in 95 % ethanol for 1 h, then put in 100 % ethanol for 3 times change, every change is 1.5 h, then put in xylene for 3 times change, 1.5 h for each change, paraffin (60 °C) for 2 changes, 2 h for every change, at last take tissues out and embed into paraffin blocks. After embedding, kidney solid blocks sent to Technical University of Munich for section and hematoxylin and eosin staining for injury analysis.

3.10 Cytokine qPCR detection

RNA isolation is performed according to QIAGEN RNeasy mini kit (QIAGEN, 74104) protocol. Briefly, kidneys are disrupted and homogenized by using iron beads by strong shake in RLT buffer. Pipette 10 µl β-mercaptoethanol in each vial with total 1 ml lysis RLT buffer inside. Centrifuge cell lysate for 3 min at 8000 g (Eppendorf). Be careful when removing supernatant by pipetting it to a clean spin column with a collection tube on the bottom. Pipette 1x volume 70% ethanol to the supernatant in the spin column, mix with 70% ethanol by pipetting. Top up with 700 µl of the sample to RNeasy spin column on the top of a collection tube. Close the lid and centrifuge at 8000 g for 20 s. Trash the flow-through after every centrifugation. Put the spin column containing RNA in RNAse-free collection tube. Pipette 20-50 µl RNase-free water to the spin column. Lock the lid and centrifuge at maximum speed for 60 s to dissolve the RNA. At last use Nanodrop to check the concentration of isolated RNA.

RNA reverse transcription is performed according to Invitrogen SuperScript III FirstStrand Sythesis System (Thermo Fisher, 18080-051) instruction. Briefly, mix the components below to a RNase-free EP tube: 0.5 µg RNA isolated from tissue, 1 µl 10 mM dNTP (10 mM each dATP, dGTP, dCTP and dTTP); 1 µl of oligo(dT) (stock concentration: 50 µM); add RNase-free and distilled water up to 13 µl. Increase temperatue to 65°C for 5 min and put samples on ice for 60 s. Short centrifugation of the EP tubes and add 4 µl 5x First-Strand Buffer, 1 µl 0.1 M DTT, 1 µl RNase Inhibitor (Takara). Mix well by careful pipetting for several times. Incubate at 50°C for 1 h. Deactivate the reaction by increasing

temperature to 70°C for 15 minutes. Then the reverse transcripted cDNA is used as a template stock, dilute template for target qPCR test.

qPCR is performed according to SYBR™ Green PCR Master Mix (Thermo Fisher, 4309155) instruction. Briefly, for each qPCR reaction, SYBR Green is added in 10 µl; forward primer and reverse primer are added according to different genes; cDNA is added in 5 µl; H_2O is added up to 20 µl for each reaction.

Table 5. qPCR primers

qPCR Primers	5´-3´
IL-10 forward	CAG AGA AGC ATG GCC CAG
IL-10 reverse	TGC TCC ACT GCC TTG CTC TT
IL-1b forward	TGG ACC TTC CAG GAT GAG GAC A
IL-1b reverse	GTT CAT CTC GGA GCC TGT AGT G
IL-6 forward	TAG TCC TTC CTA CCC CAA TTT CC
IL-6 reverse	TTG GTC CTT AGC CAC TCC TTC
IL-18 forward	GAC AGC CTG TGT TCG AGG ATA TG
IL-18 forward	TGT TCT TAC AGG AGA GGG TAG AC
KIM-1 forward	CTG GAA TGG CAC TGT GAC ATC C
KIM-1 reverse	GCA GAT GCC AAC ATA GAA GCC C
L-FABP forward	AGG AGT GCG AAC TGG AGA CCA T
L-FABP reverse	GTC TCC ATT GAG TTC AGT CAC GG
TNF-a forward	GGT GCC TAT GTC TCA GCC TCT T
TNF-a reverse	GCC ATA GAA CTG ATG AGA GGG AG

3.11 Ischemia reperfusion induced AKI

Kidney unilateral ischemia reperfusion injury induction was operated in collaboration with Prof. Hans-Joachim Anders under their regulations. 8-14 weeks old Clec9a^{cre}CD64^{iDTR} mice were anesthetized before surgery by using a master mix with medetomidine, midazolam and fentanyl inside, plus rectal temperature with online detecting for every mouse. Anesthetized mice were put on a adjustable temperature plate to keep mouse body temperature around 37 °C. Flank incision was operated and the renal hilum of the left kidney was clamped for 25 min by using a small aneurysm clamp. The temperature check is applied during whole operation process. After ischemia surgery, successful injury induction was reflected by mouse kidney color changing from pale white to normal and also successful wake-up of mice. To close the wound, peritoneal and cutaneous layer of skin and muscle were stitched with absorbable sutures. 1 day or 5 days after operation kidneys were taken for FACS analysis.

3.12 Glomerular filtration rate (GFR) detection

GFR measurement is performed according to Prof. Hans-Joachim Anders´s protocol. Briefly, on day -3 GFR is measured as baseline, day 0 GFR is measured to check if DT injection will lead to GFR change, day 1 and day 5 GFR are measured for evaluating if CD64^{+} MPs depletion will lead to injury severity change compare with control. Clec9a^{cre}CD64^{iDTR} mice were firstly anesthetized with isoflurane holder supplied with oxygen, then blazer was used to remove the hair on the back and tightly attach GFR detection device on the back (MediBeacon). The recording time started from injection of FITC-sinistrin (eye injection, 150 mg/kg body weight) and last for 2 h. In order to detect the baseline GFR value, the signal was recorded for 5-10 min before FITC-sinistrin injection. MPD Studio software (MediBeacon) was used for GFR analysis. GFR (µl/min per 100 g body weight) was calculated from Prof. Hans-Joachim lab’s protocol.

3.13 Cell sorting

Cell sorting is performed according to Flow cytometry core facility of LMU. Briefly, after kidney immune cells are isolated after percoll and stained with sorting panel, BMDC is also stained with sorting panel, FACSAria Fusion are used for sorting. After drop and gap adjustment, 100 µm nozzle is used for $CD64^+$ MPs sorting. In the sort layout, select 4-Way purity model to sort. During sorting, monitor the efficiency in the sort layout window and kept at an optimal level by adjusting the flow rate.

3.14 In vitro MP histone stimulation

After sorting, $CD64^+$ MPs from each are split into 3 U-plate wells, each well contains 30 µl complete RPMI, BMDC and sorted $F4/80^{hi}$ cells are seeded for 10,000 cells/well. BMDC are treated with conditions: w/o treatment; histone (50 µg/ml); zymosan (10 µg/ml). Sorted $F4/80^{hi}$ cell are treated with conditions: w/o treatment; zymosan (10 µg/ml); histone (50 µg/ml). Incubate overnight and collect supernatant for cytokine analysis.

3.15 Cytokine Legendplex detection

Cytokine detection is done according to Legendplex instruction (Biolegend, 740150). In this kit, this panel can measure 13 mouse cytokines, including IL-1β, IL-1α, IL-10, IL-12p70, IL-17A, IL-6, IL-27, IL-23, CCL2 (MCP-1), IFN-γ, IFN-β, GM-CSF, and TNF-α. For all the reagents in the kit must be store at room temperature before use. 8 standard points are prepared, C7 is highest concentration, C0 is lowest concentration (assay buffer), dilution factor is 4. Supernatant from $CD64^+$ MPs after histone in vitro stimulation is collected diluted 2-fold with assay buffer before test. After beads incubation and antibody incubation, the samples are used for FACS analysis, and the results are analyzed by online tool (QOGNIT).

3.16 Statistical analysis

Statistics was analyzed by using unpaired student's t-test in Prism 8 software (GraphPad). One-way and Two-way ANOVA were used for multiple comparisons. P-value < 0.05 was considered significant, and p-value < 0.01 was considered very significant.

3.17 Antibody list

Table 6. List of used antibodies

Gene name	Fluorophore	Producer	Clone	Dilution factor
CD3ε	PeCy5	BioLegend	145-2C11	1:300
CD4	BUV737	BD Biosciences	GK1.5	1:200
CD8a	PerCPCy5.5	BioLegend	53-6.7	1:200
CD11b	BV421	BioLegend	M1/70	1:300
CD11b	BUV737	BD Biosciences	M1/70	1:800
CD11c	BV785	BioLegend	N418	1:200
CD16/CD32	purified	BD Biosciences	N418	1:300
CD19	BV650	BioLegend	6D5	1:200
CD24	BUV395	BD Biosciences	M1/69	1:400

CD45.2	PeCy7	BioLegend	104	1:300
CD45R/B220	FITC	BioLegend	RA3-6B2	1:200
CD45R/B220	PE	BioLegend	RA3-6B2	1:200
CD64 (FcγRI)	PE	BioLegend	X54-5/7.1	1:200
F4/80	AF647	BioLegend	BM8	1:300
I-A/I-E (MHCII)	BV421	BioLegend	M5/114.15.2	1:300
I-A/I-E (MHCII)	AF700	BioLegend	M5/114.15.2	1:300
Ly-6C	BV605	BioLegend	HK1.5	1:200
Ly-6G	PerCPCy5.5	BioLegend	1A8	1:200
XCR1	BV421	BioLegend	ZET	1:100
FOXP3	AF647	BioLegend	MF-14	1:200
ROR gamma (t)	BV421	BioLegend	Q31-378	1:100
T-bet	PE	BioLegend	4B10	1:100
Mouse IgG	PE	BioLegend	MOPC-21	1:200

Mouse IgG	BV421	BioLegend	MPC-11	1:100
Mouse IgG	AF647	BioLegend	MPC-11	1:200

4 Results

4.1 MPs with Clec9a expressing history play important role in cisplatin induced AKI

4.1.1 BUN and creatinine increased in Clec9acreRosaYFP mice after 48 hours cisplatin treatment

To determine the function of MPs with Clec9a expressing history in cisplatin induced AKI, we treated Clec9a^{cre}Rosa^{YFP} mice with NaCl or cisplatin and analyzed 48 hours later. We firstly checked BUN and creatinine to confirm the injury induction after 48 hours of cisplatin treatment. It showed BUN and creatinine increased very significantly in mice injected with cisplatin compare with NaCl treated mice, indicating injury is successfully induced.

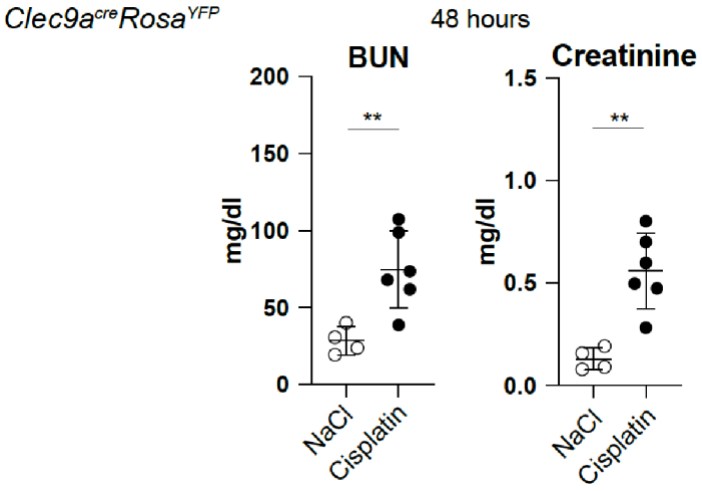

Fig. 2. Serum creatinine and BUN increased after 48 hours cisplatin treatment. Clec9a^{cre}Rosa^{YFP} mice were injected with NaCl or cisplatin and then used analyzed 2 days later. Creatinine and BUN from serum are measured after 2 days. Each dot represents one

mouse. ** p<0.01. Student's t test. Data from 2 independent experiments. (Modified from Salei et al., 2021)

4.1.2 cDC1 and cDC2 are lost from inflamed kidney

In order to check leukocyte dynamics in Clec9a^{cre}Rosa^{YFP} mice treated with cisplatin for 48 hours, we used flow cytometry to profile each immune subset in the kidney. The gating strategy for kidney immune cells is shown (Fig. 3A). It showed that cDC1 and cDC2 decreased significantly both in counts (Fig. 3B) and frequency (Fig. 3C) in cisplatin treated mice compare with NaCl treated mice. Neutrophil as the early sign of inflammation is increased in frequency (Fig. 3C). Other populations do not have significant change. Since we saw cDC1 and cDC2 are lost from cisplatin treated mice, and cDC1/cDC2 are 2 major components of MPs with Clec9a expressing history, we hypothesized not just these 2 populations but all MPs with Clec9a expressing history may have important functions in cisplatin induced AKI.

A

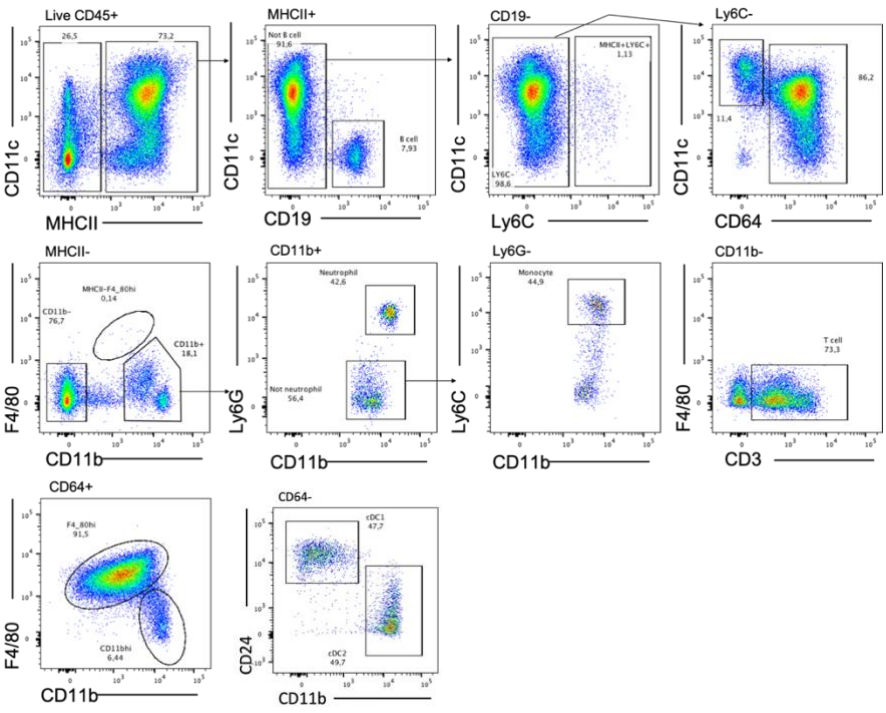

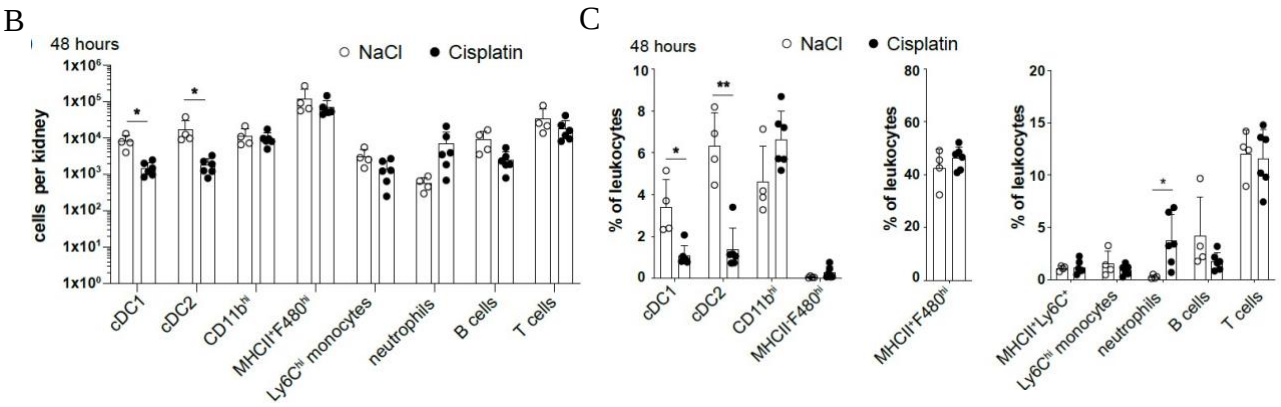

Fig. 3. MPs with Clec9a-expression history in cisplatin induced AKI for 48 hours. (A) Representative gating of kidney leukocytes. Live cells from CD45.2$^+$ gating were gated as MHCII$^-$ and MHCII$^+$ cells as indicated. MHCII$^+$CD19$^+$ cells are B cells. cDC2 and cDC1 were distinguished from CD11c$^+$CD64$^-$ cells and CD64$^+$ cells were subdivided into CD11b^{hi} and F4/80^{hi} MPs. CD11b and F4/80 were used to identify MHCII$^-$F4/80^{hi} MPs, MHCII$^-$CD11b$^+$ cells were subdivided into monocytes and neutrophils. MHCII$^-$CD11b$^-$ cells are T cells. (B, C) The cell counts (B) and frequency (C) per kidney of the indicated immune subsets gated 48 hours after cisplatin treatment. Each dot represents one mouse. * $p<0.05$, ** $p<0.01$. Student's t test. Data from 2 independent experiments. (Modified from Salei et al., 2021)

4.2 Depletion of MPs with Clec9a expressing history increases kidney injury

4.2.1 cDC1, cDC2 and CD64+ MPs depletion increases injury severity after cisplatin treatment for 48 hours

To investigate if MPs with Clec9a expressing history may have function in cisplatin induced AKI, we decided to deplete these MPs and induce AKI to check kidney injury severity. In order to do that, we firstly constructed a depletion model by crossing Clec9a^{cre} line with Rosa^{iDTR} line to get Clec9a^{cre}Rosa^{iDTR} mice, in this model all MPs with Clec9a expressing history will be depleted after DT injection. We injected DT for 24 hours to deplete MPs, and then injected cisplatin to induce AKI for 48 hours. After 48 hours, we sacrificed mice for analysis. It showed BUN and creatinine are increased in both control mice (Clec9a^{wt}Rosa^{iDTR} injected with DT and Clec9a^{cre}Rosa^{iDTR} injected with PBS) and MP-

depleted mice (Clec9a^{cre}Rosa^{iDTR} injected with DT) compare with baseline (NaCl treated mice), indicating successful injury induction. By comparing BUN and creatinine in control mice and depletion mice we saw BUN and creatinine increased in MP-depleted mice, meaning MPs with Clec9a expressing history have protective role in cisplatin induced AKI (Fig. 4A). We then profiled all immune cell subsets by using flow cytometry. cDC1, cDC2, CD11b^{hi} and F4/80^{hi} cells in MP- depleted mice decreased significantly both in cell counts and frequency compared with control mice, MHCII^{-}F4/80^{hi} cells increased in counts and frequency in MP-depleted mice due to downregulation of MHCII on F4/80^{hi} cells (Fig. 4B). Beside MPs with Clec9a expressing history, Ly6C^{hi} monocytes increased in counts and frequency in depleted mice, infiltrated MHCII^{+}Ly6C^{hi} monocytes decreased in counts in depleted mice, neutrophils as mark of inflammation increased in frequency in MP-depleted mice (Fig. 4B and C). In conclusion, depletion of MPs with Clec9a expressing history will lead to more severe injury, indicating all these cells together have protective role in cisplatin induced AKI.

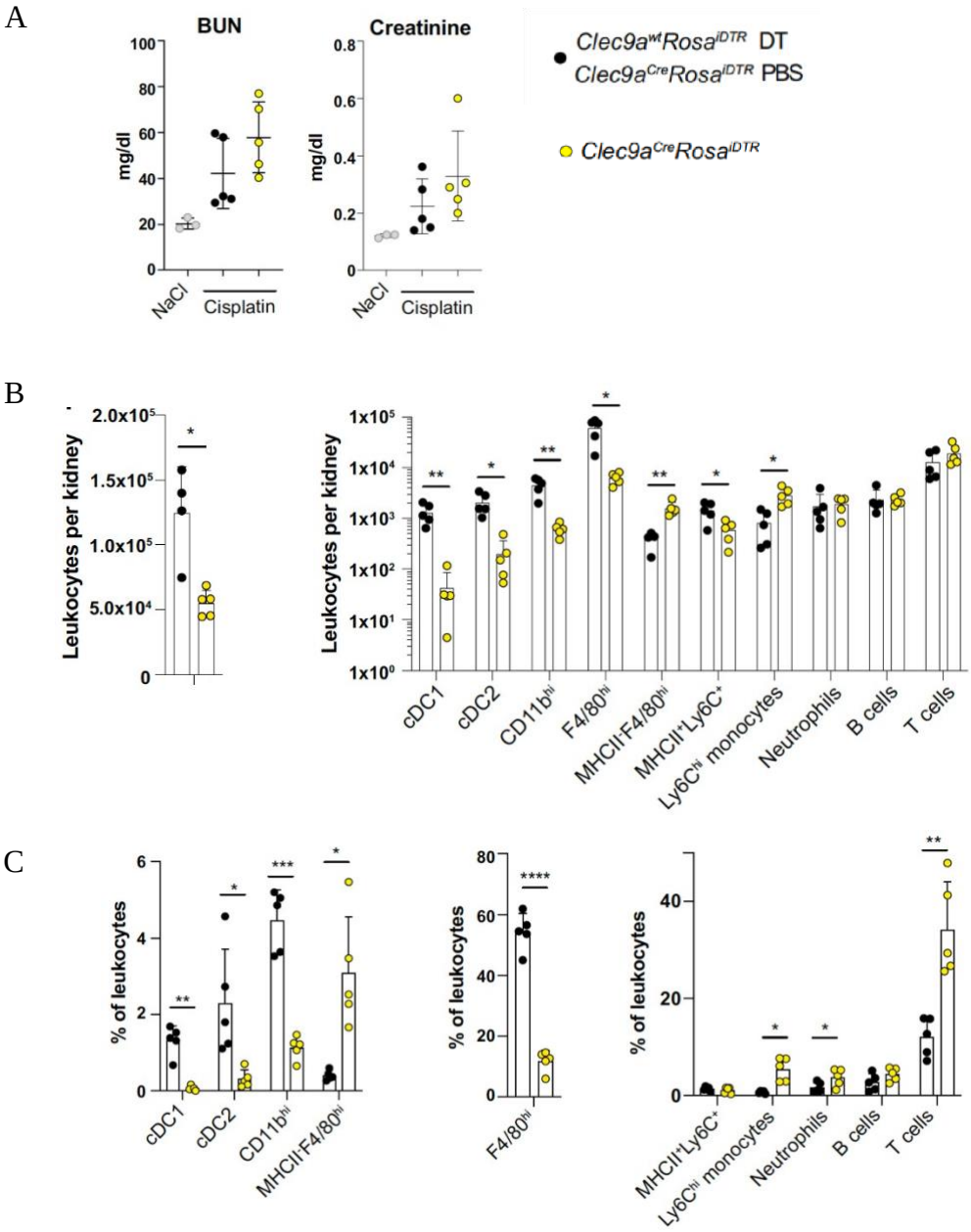

Fig. 4. MPs with Clec9a-expression depletion leads to increased AKI severity.

(A-C) Clec9a^{cre}Rosa^{iDTR} or Clec9a^{wt}Rosa^{iDTR} mice were injected with DT and then treated with cisplatin for 48 hours. (A) BUN and creatinine levels. (B, C) Kidney total leukocytes (B), cell counts and frequency (C) were indicated. *P < 0.05, **P < 0.01, ***P < 0.001, and ****P < 0.0001. One-way ANOVA for (A), student's t test for (B) and (C). Data from 2 independent experiments. (Modified from Salei et al., 2021)

4.3 cDC1 depletion in steady state is efficient and specific

4.3.1 cDC1 is efficiently and specifically depleted in XCR1-venus-DTR mice after DT injection for 24 hours

cDC1 is a major part of MPs with Clec9a expressing history, to investigate cDC1´s function in cisplatin induced AKI, we will use XCR1-venus-DTR model to specifically deplete cDC1 and then induce AKI. We firstly checked cDC1 depletion efficiency and specificity in steady state. XCR1-venus-DTR mice were injected with PBS or DT respectively, 24 hours after DT injection we collected kidneys for FACS analysis. Gating strategy is shown below (Fig. 5A). The results showed cDC1 counts and frequency decreased significantly in DT injected mice compared with PBS injected mice, and other immune populations do not change neither in cell counts and frequency (Fig. 5B, C and D), indicating this model has high depletion efficiency and specificity.

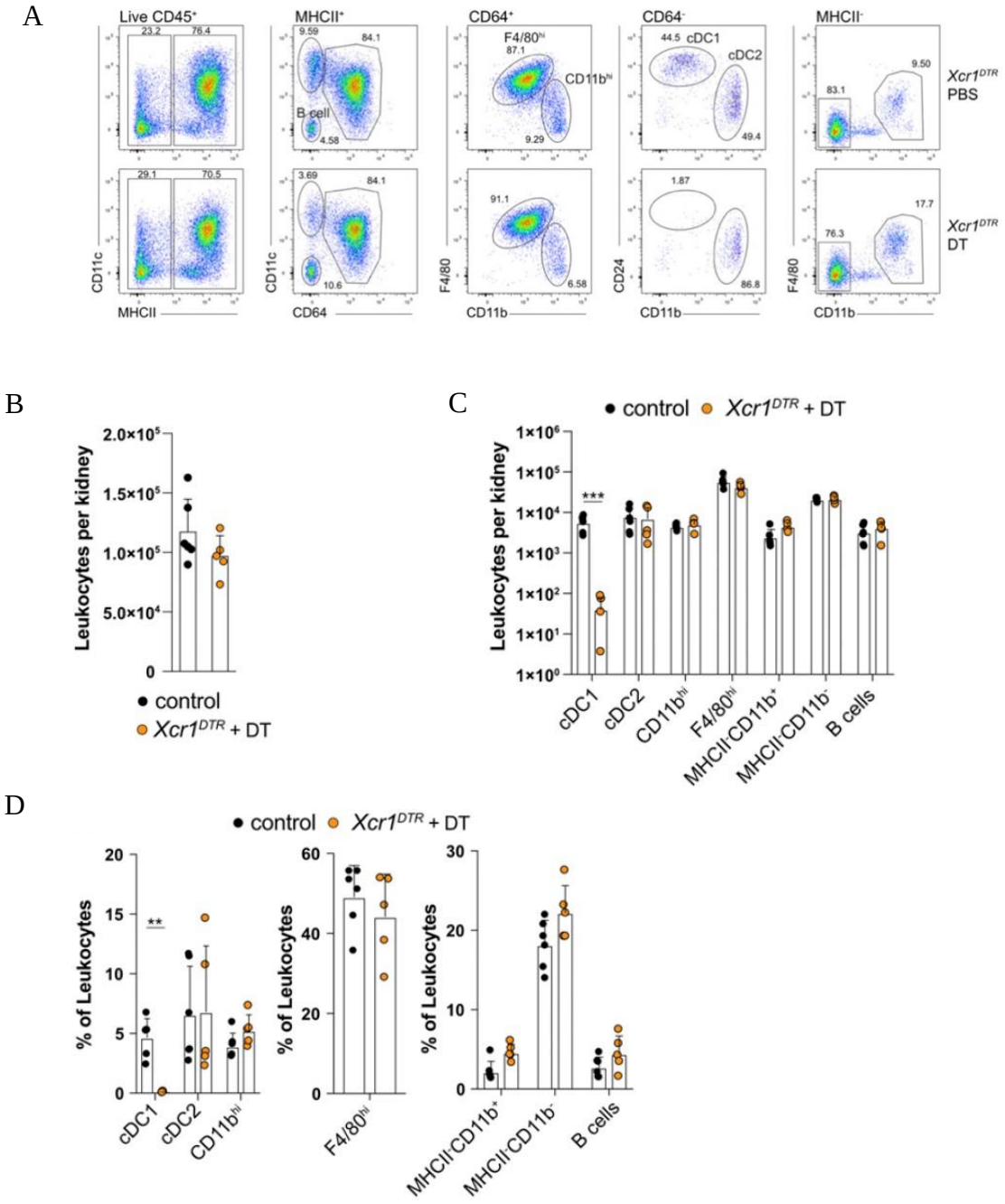

Fig. 5. cDC1 is depleted efficiently and specifically in XCR1-venus-DTR mice after DT injection for 24 hours. XCR1-venus-DTR$^{w/k}$ mice were injected with DT to deplete cDC1, XCR1-venus-DTR$^{w/k}$ were control mice injected with PBS. (A) CD45.2^{+} MHCII^{+} live cells were gated and further subdivided into CD11c^{+} CD64^{+}, CD64^{-} cells, and CD11c^{-}CD64^{-} cells are B cells. cDC2 and cDC1 were distinguished in the CD11c^{+} CD64^{-} gating. CD64^{+} cells were further subdivided into F4/80^{hi} and CD11b^{hi} MPs. MHCII^{-} cells were subdivided into neutrophils, monocytes, and T cells. (B) Total leukocytes in one kidney. (C) All

immune subsets count in one kidney. (D) All immune subsets frequency in one kidney. **P < 0.01, and ***P < 0.001. Student's t test. Data from 2 independent experiments. (Modified from Salei et al., 2021)

4.4 cDC2 depletion does not influence the severity of cisplatin induced AKI

4.4.1 cDC2 is reduced in Clec9a^{cre}IRF4$^{f/f}$ mice and other immune cell subsets do not change compare with littermate controls

IRF4 is an important transcription factor for cDC2 migrating to lymph nodes to prime T cells, and loss of IRF4 inhibits cDC2 development and its function (80, 81). In order to investigate cDC2´s function in cisplatin induced AKI, we firstly analyzed if cDC2 is reduced in Clec9a^{cre}IRF4$^{f/f}$ mice compare with littermates. As expected, cDC2 is decreased in frequency in Clec9a^{cre}IRF4$^{f/f}$ mice compare with littermate controls and other leukocytes were not altered (Fig. 6 A, B and C).

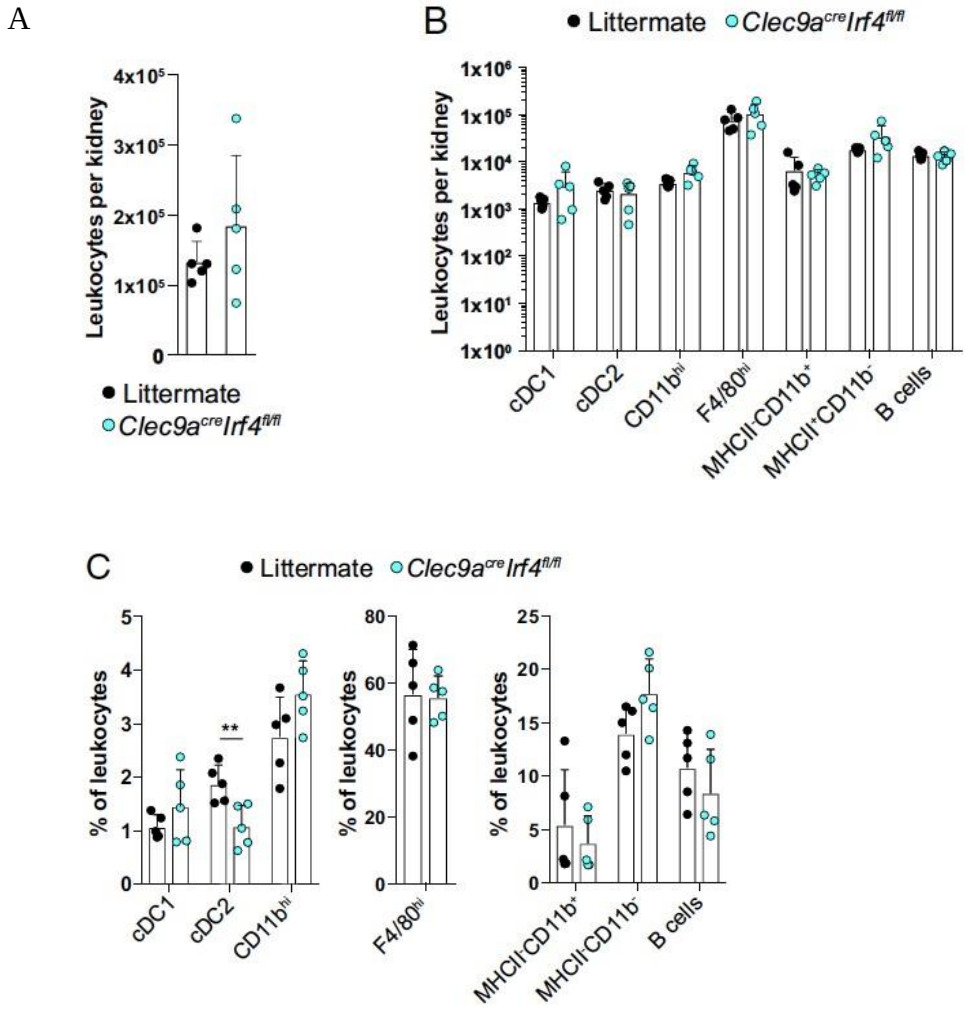

Fig. 6. cDC2 is reduced in Clec9acreIRF4f/f mice but other immune subsets do not alter. Clec9a^{cre}IRF4$^{f/f}$ and littermate control mice were analyzed by using FACS analysis. (A-C) The total kidney leukocytes, number and frequency of the indicated immune subsets in kidney were indicated. (A) Total leukocytes per kidney. (B) All immune subsets count in kidney. (C) All immune subsets frequency in kidney. **P <

0.01. Student's t test. Data from 2 independent experiments. (Modified from Salei et al., 2021)

4.4.2 BUN and creatinine do not change after cisplatin treatment for 72 hours in Clec9a^{cre}IRF4$^{f/f}$ mice

To investigate severity of AKI after cDC2 ablation in Clec9a^{cre}IRF4$^{f/f}$ mice, we induced AKI in Clec9a^{cre}IRF4$^{f/f}$ mice and Clec9a^{wt}IRF4$^{f/f}$ mice, 72 hours later we measured serum BUN and creatinine. It showed BUN and creatinine do not change in Clec9a^{cre}IRF4$^{f/f}$ mice

compare with Clec9a^{wt}IRF4$^{f/f}$ after cisplatin injection for 72 hours, indicating cDC2´s function in cisplatin induced AKI is minor.

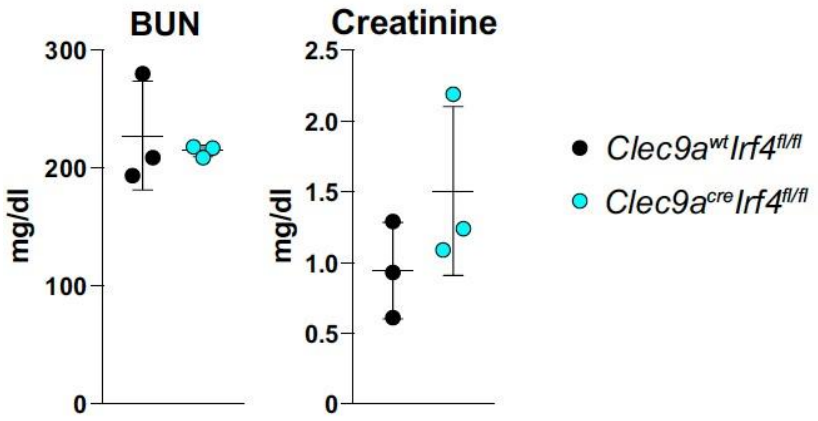

Fig. 7. Clec9acreIRF4f/f mice do not show altered susceptibility to cisplatin-induced AKI. Mice were injected with cisplatin by 20 mg/kg body weight and serum creatinine and BUN were analyzed 72 hours later. Student's t test. (Modified from Salei et al., 2021)

4.5 CD64^{+} MPs are efficiently and specifically depleted in Clec9a^{cre}CD64^{iDTR} mice in steady state

4.5.1 CD64^{+} MPs are depleted in kidney without affecting kidney function and architecture for 24 hours in steady state

In order to deplete CD64^{+} MPs in kidney, we used a depletion model Clec9a^{cre}CD64^{iDTR} mice generated by Dalia Pakalniskyte during her PhD, in this model only cells have Clec9a expressing history and also expressing CD64 will be depleted when injected with DT. We firstly injected with Clec9a^{cre}CD64^{iDTR} mice with DT, 24 hours later we collected kidneys for FACS analysis. Gating strategy is shown (Fig. 8A). It showed CD64^{+} MPs are efficiently and specifically depleted without affecting other immune populations (Fig. 8B and C). Interestingly, DT treatment of Clec9a^{cre}CD64^{iDTR} mice caused a significant increase in infiltrated MHCII^{+}Ly6C^{+} cells which could be attributed to newly opened niche given by CD64^{+} MPs (Fig. 8B and C). Loss of CD64^{+} MPs were double checked by microscopy, as shown with about fourfold reduction of F4/80^{hi} cells in the kidney cortex and about 2-fold reduction in the kidney medulla in DT-treated Clec9a^{cre}CD64^{iDTR} mice (Fig. 8D). Since CD64^{+} MPs is a major MP population localized in kidney, we were wondering if sudden depletion will lead to kidney damage, so we checked BUN and creatinine and also used PAS staining to check the kidney architecture after depletion. It showed CD64^{+} MPs depletion did not induce significant change in BUN and creatinine, and PAS scoring indicated the kidney architecture did not have significant alteration after CD64^{+} MPs depletion (Fig. 8E and F).

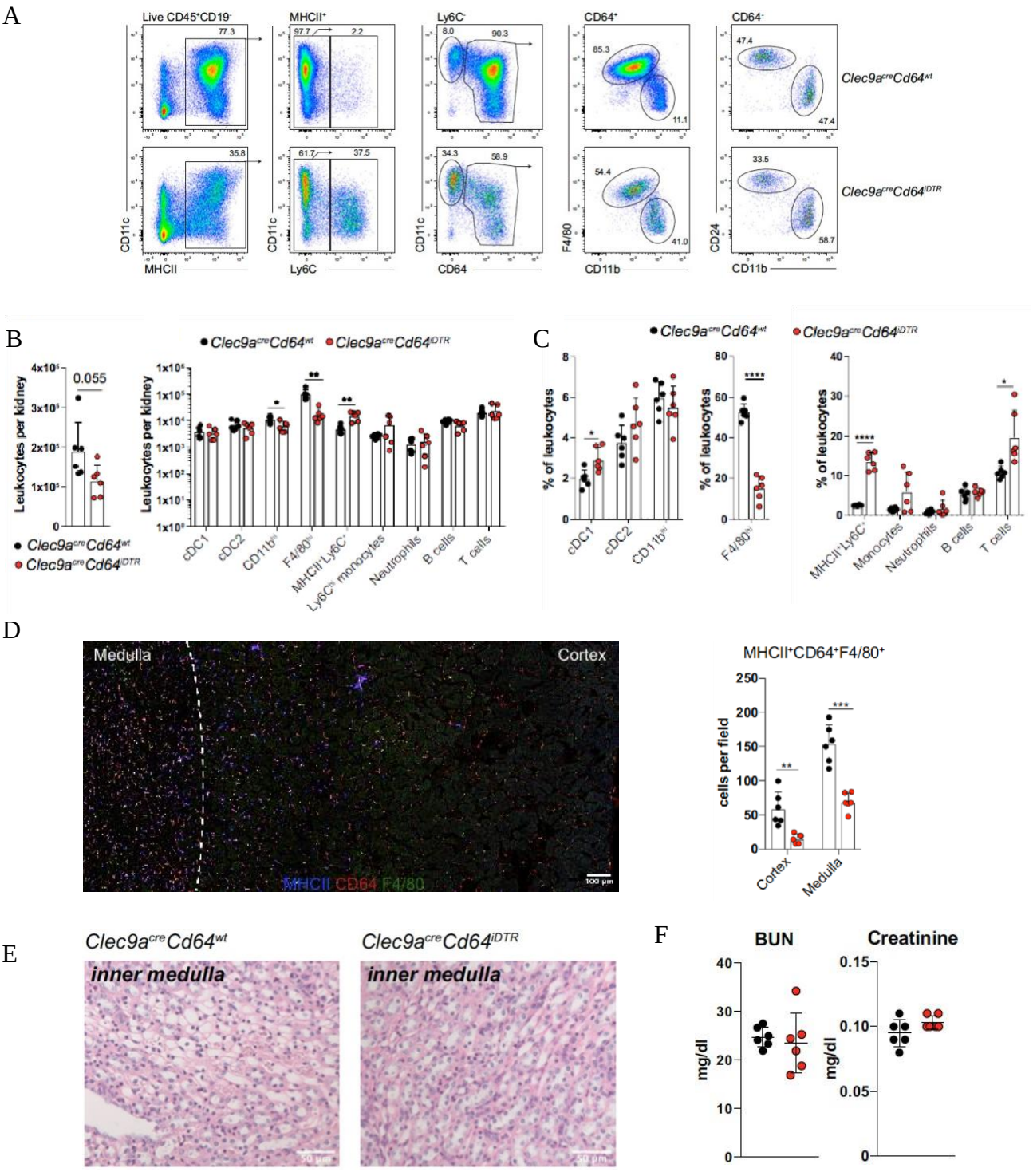

Fig. 8. Clec9acreCD64iDTR mice allow for specific depletion of renal CD64+ MPs, kidney function and architecture do not change after CD64+ MPs depletion. (A–F) Clec9a$^{wt/cre}$CD64^{iDTR} and Clec9a$^{wt/cre}$CD64^{wt} mice were i.p. injected with DT and analyzed 24 hours later. (A) The kidney immune cells were analyzed by using flow cytometry. CD45.2^{+}MHCII^{+} live cells were firstly gated out and subdivided into 2 populations according to Ly6C expression. Ly6C$^{–}$ cells were further subdivided into CD11c^{+}CD64^{+} and

$CD11c^{+}CD64^{-}$ cells, in the $CD11c^{+}CD64^{-}$ gating cDC1and cDC2 were distinguished by $CD24^{+}$ and $CD11b^{+}$ expression. Then $CD11c^{+}CD64^{+}$ cells were subdivided into $F4/80^{hi}$ and $CD11b^{hi}$ MPs. Total kidney leukocytes, other immune cell subsets number (B) and frequency (C) of each kidney are plotted. (D) The kidney cryosections of DT injected $Clec9a^{wt/cre}CD64^{iDTR}$ and $Clec9a^{wt/cre}CD64^{wt}$ mice were stained for CD64, MHCII, and F4/80, CD64 is shown in red, MHCII is shown in blue, F4/80 is shown in green. The number of $CD64^{+}$ MPs of each field in both kidney cortex and medulla were calculated and were plotted by adding up together of each 6 fields. Scale bar is 100 µm. (E) The normal kidney inner medulla architecture in control mice and DT-treated $Clec9a^{wt/cre}CD64^{iDTR}$ mice. PAS staining of renal medulla 24 hours after DT administration. Scale bar is 50 µm. (F) Serum creatinine and blood urea nitrogen (BUN) in DT-treated control mice and $Clec9a^{wt/cre}CD64^{iDTR}$ mice after 24 hours. *P < 0.05, **P < 0.01, and ****P < 0.0001. Student's t test. Data from 2 independent experiments. (Modified from Salei et al., 2021)

4.5.2 Immune populations are not affected in spleen after renal CD64+ MPs depletion

To investigate the depletion specificity of $Clec9a^{cre}CD64^{iDTR}$ mice after DT injection, we used flow cytometry to analyze immune cell subsets in the spleen. Gating strategy is shown (Fig. 9A). It is shown all of the immune populations did not change in cell counts and frequency after DT injection in spleen (Fig. 9B and C), indicating this model will not induce unspecific depletion such as red pulp macrophages (RPM) depletion in spleen, since RPM also express CD64 but without Clec9a expression history.

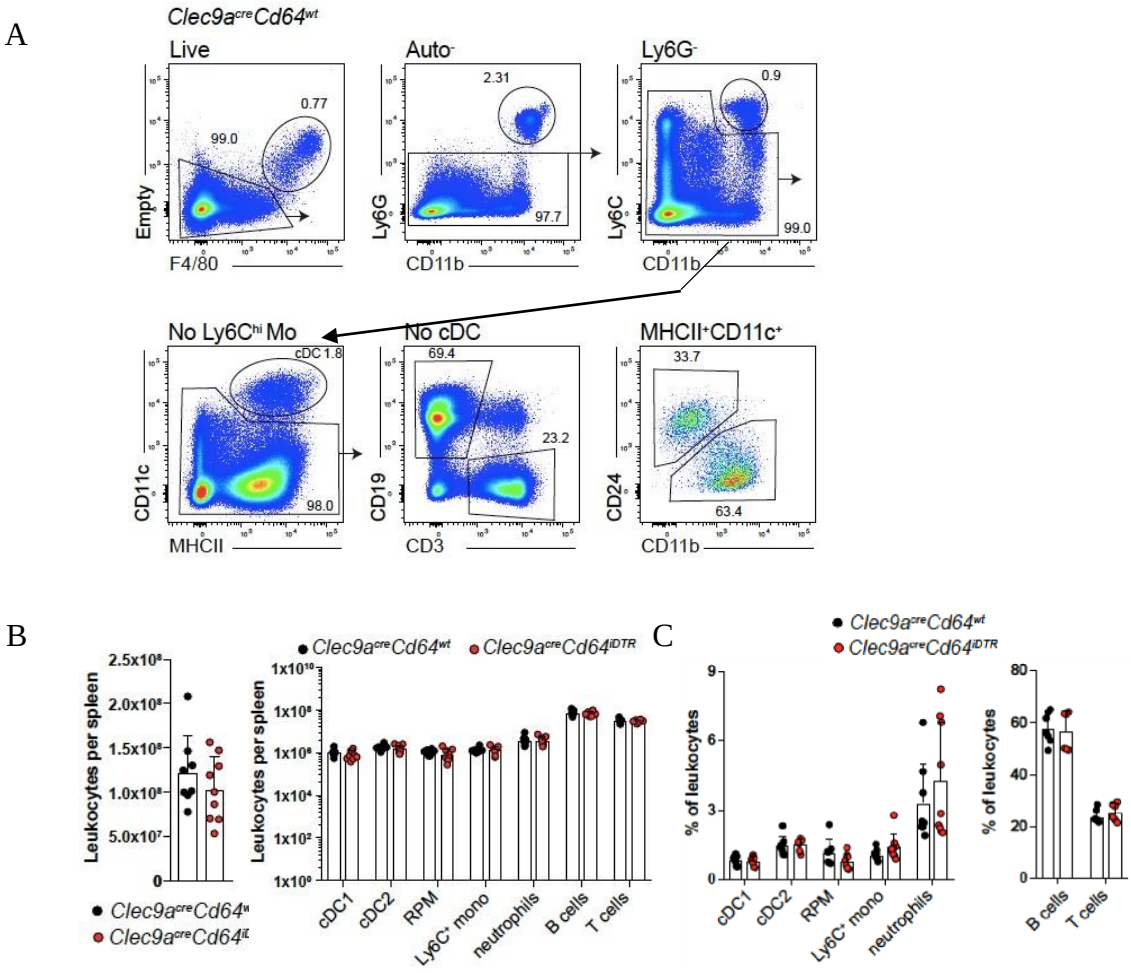

Fig. 9. No alterations of leukocyte populations in spleen from DT treated Clec9a^{cre}CD64^{iDTR} mice. (A–C) Clec9a$^{wt/cre}$CD64^{iDTR} and Clec9a$^{wt/cre}$CD64^{wt} mice were i.p. injected with DT and analyzed 24 hours later. (A) Single live cells were gated. Autofluorescent F4/80^{+} cells were defined as red pulp macrophages (RPM). Autofluorescence negative cells were further analyzed for presence of Ly6G^{+}CD11b^{+} neutrophils and Ly6G^{-}Ly6C^{hi}CD11b^{+} monocytes. cDCs were defined as CD11c^{+} and MHCII^{+} cells and further subset into cDC1 and cDC2 according to CD24 and CD11b expression. B cells were defined as CD19^{+} cells, T cells were defined as CD3^{+} cells. Total immune cells in spleen, cell number (B) and frequency (C) of indicated populations per spleen were quantified. Student's t test. Data from 2 independent experiments. (Modified from Salei et al., 2021)

4.6 CD64$^+$ MPs depletion increases kidney injury severity after cisplatin treatment

4.6.1 CD64$^+$ MPs kept depleted post cisplatin treatment for 48 hours

To investigate CD64$^+$ MPs function in cisplatin induced AKI, we injected mice with PBS or DT according to different genotypes, 24 hours later we injected NaCl or cisplatin. NaCl injected mice are baseline control. 48 hours after cisplatin treatment, we sacrificed mice for analysis (Fig. 10A). We firstly checked each immune population in kidney, it showed in depleted mice CD64$^+$ MPs cell kept depleted after 48 hours post cisplatin injection, cDC2 and MHCII$^+$Ly6C$^+$ infiltrated monocytes decreased in cell counts (Fig. 10B and C). cDC1, Ly6C$^+$ monocytes, neutrophils, T cells and B cells are increased in frequency in depleted mice, it could be attributed to the decrease of leukocytes that makes the normalization number bigger (Fig. 10D).

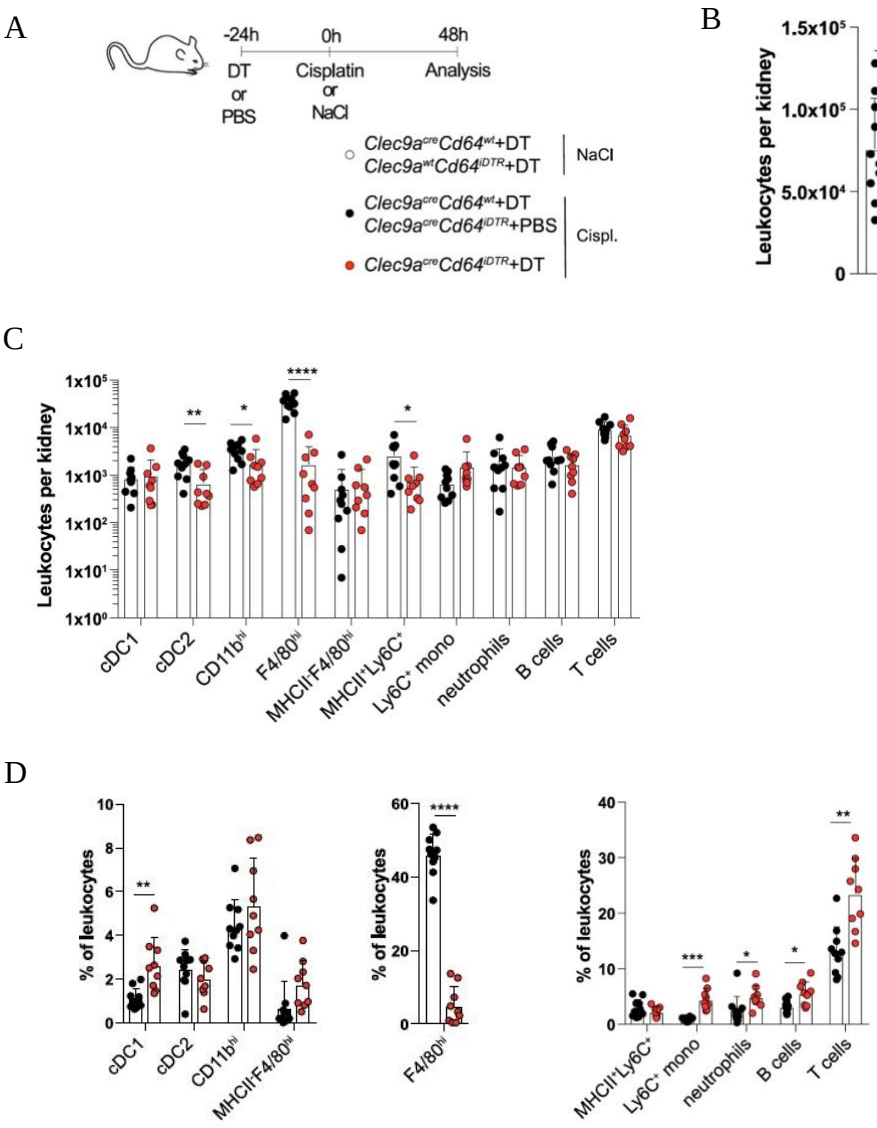

Fig. 10. CD64⁺ MPs kept depleted in Clec9a^{cre}CD64^{iDTR} after 24 hours DT injection and 48 hours cisplatin injection. Clec9a^{cre}CD64^{iDTR} mice and Clec9a^{cre}CD64^{wt} mice were i.p. injected with DT or PBS, 24 hours later mice were injected with NaCl or cisplatin, 48 hours later all mice were sacrificed for analysis. **(**A) Experimental design. (B) Leukocytes per kidney. (C) Immune population cell counts per kidney. (D) Immune population frequency of leukocytes. Open circle represents Clec9a^{cre}CD64^{wt} mice or Clec9a^{cre}CD64^{iDTR} mice injected with DT and NaCl, closed circle represents Clec9a^{cre}CD64^{wt} or Clec9a^{cre}CD64^{iDTR} injected with DT/PBS and cisplatin, red circle represents Clec9a^{cre}CD64^{iDTR} mice injected with DT and cisplatin. *P < 0.05, **P < 0.01, ***P < 0.001, ****P < 0.0001, and only statistically significant differences are indicated. Student's t test. Data from 3 independent experiments. (Modified from Salei et al., 2021)

4.6.2 Injury severity is increased in CD64$^+$ MPs depleted mice

To investigate if CD64$^+$ MPs depletion leads to more severe injury in AKI, we checked BUN and creatinine after depletion and cisplatin treatment. It showed BUN is increased in CD64$^+$ MPs depleted mice, indicating CD64$^+$ MPs protective role in AKI (Fig. 11A). However, creatinine does not change significantly in CD64$^+$ MPs depleted mice, it could be attributed to the reason at this time point creatinine is not sufficient to reflect kidney injury severity (Fig. 11A). Caspase 3 is a lysosomal enzyme produced in cell apoptosis, it is another marker for evaluating injury in this model, we found CD64$^+$ MPs depleted mice have a significant increase of caspase 3 compared with control, indicating severer injury in these mice and also proved CD64$^+$ MPs can protect kidney in cisplatin induced AKI (Fig. 11B). Kidney injury marker KIM-1 is usually used to evaluate the injury severity. To check if injury is successfully induced by cisplatin, we firstly checked kidney KIM-1 in both control mice and CD64$^+$ MPs depleted mice by qPCR, we found all cisplatin injected mice were increased in KIM-1 expression. Since KIM-1 is phosphatidylserine receptor expressed on cells undergoing apoptosis, and it can inhibit inflammatory cytokines produced to dampen inflammation from epithelial cells (82), we found KIM-1 is decreased in CD64$^+$ MP depleted mice, indicating more sever inflammation happening after depletion (Fig. 11C).

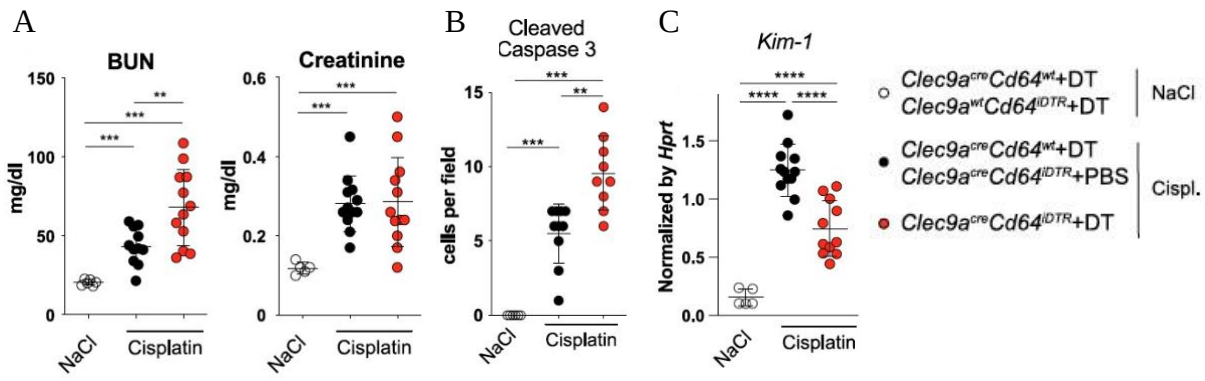

Fig. 11. CD64^{+} MPs depletion increased AKI severity. Clec9a^{cre}CD64^{iDTR} mice and Clec9a^{cre}CD64^{wt} mice were injected with DT or PBS, 24 hours later mice were injected with NaCl or cisplatin, 48 hours later all mice were sacrificed for analysis. (A) BUN and creatinine level are shown. (B) Cleaved caspase 3 in kidney was analyzed by immunohistochemistry staining. (C) KIM-1 mRNA was analyzed by qPCR. Open circle represents Clec9a^{cre}CD64^{wt} mice or Clec9a^{cre}CD64^{iDTR} mice injected with DT and NaCl, closed circle represents Clec9a^{cre}CD64^{wt} or Clec9a^{cre}CD64^{iDTR} injected with DT/PBS and cisplatin, red circle represents Clec9a^{cre}CD64^{iDTR} mice injected with DT and cisplatin. Each dot represents one mouse. Multiple comparison was performed by using One-way ANOVA with Bonferroni correction. Horizontal bars represent mean, error bars represent SD, *P < 0.05, **P < 0.01, ***P < 0.001, ****P < 0.0001, and only statistically significant differences are indicated. Data are combined from three independent experiments. (Modified from Salei et al., 2021)

4.6.3 Clec9a expression history is found on cDC1, cDC2, CD11b^{hi} and F4/80^{hi} cells after cisplatin treatment

To check if cisplatin can induce unexpected labeling of cells that do not have Clec9a expression history such as Ly6C^{hi} monocytes, neutrophils, B cells and T cells, we injected cisplatin into Clec9a^{cre}Rosa^{YFP} mice and 2 days later we analyzed the YFP labeling in all immune populations. Our results showed that YFP labeling is only found in cDC1, cDC2, CD11b^{hi} and F4/80^{hi} cells. This time we did not see MHCII^{-}F4/80^{hi} cells appeared in the kidney.

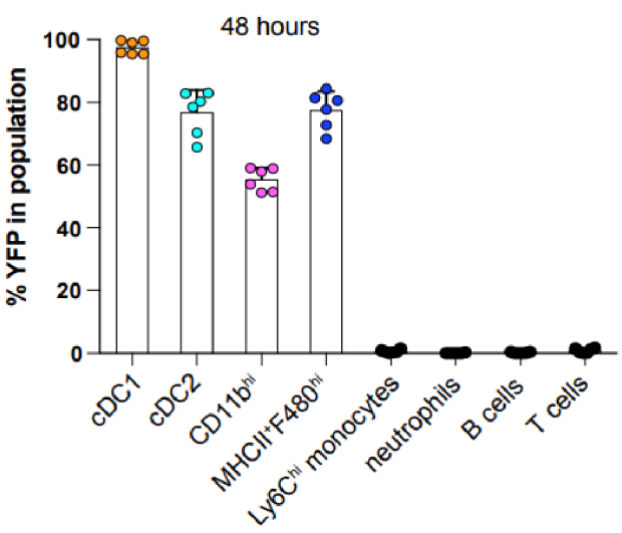

Fig 12. Clec9a expression history of MPs post cisplatin injection for 2 days. Clec9a^{cre}Rosa^{YFP} mice were i.p. injected with cisplatin or NaCl and analyzed 2 days later. YFP percentage of positive cells in the immune cell subsets 48 hours after administration. Data from 2 independent experiments. (Modified from Salei et al., 2021)

4.6.4 Cisplatin does not induce CD64 expression on immune cell populations that normally do not express it

To investigate if cisplatin can induce CD64 expression on immune cell subsets which usually do not express and would subsequently be depleted in Clec9a^{cre}CD64^{iDTR} mice we checked CD64 expression on all renal immune populations in Clec9a^{cre}Rosa^{YFP} mice injected with cisplatin for 48 hours. Our results showed that except cells expressing CD64 in steady state, such as F4/80^{hi} cells, CD11b^{hi} cells and monocytes, the rest of the populations cDC1, cDC2, neutrophils, B cells and T cells do not upregulate CD64 expression after cisplatin treatment. Considering only F4/80^{hi} cells and CD11b^{hi} cells have Clec9a expressing history among all CD64 expressing cells, we concluded the depletion is strictly happening in these 2 populations.

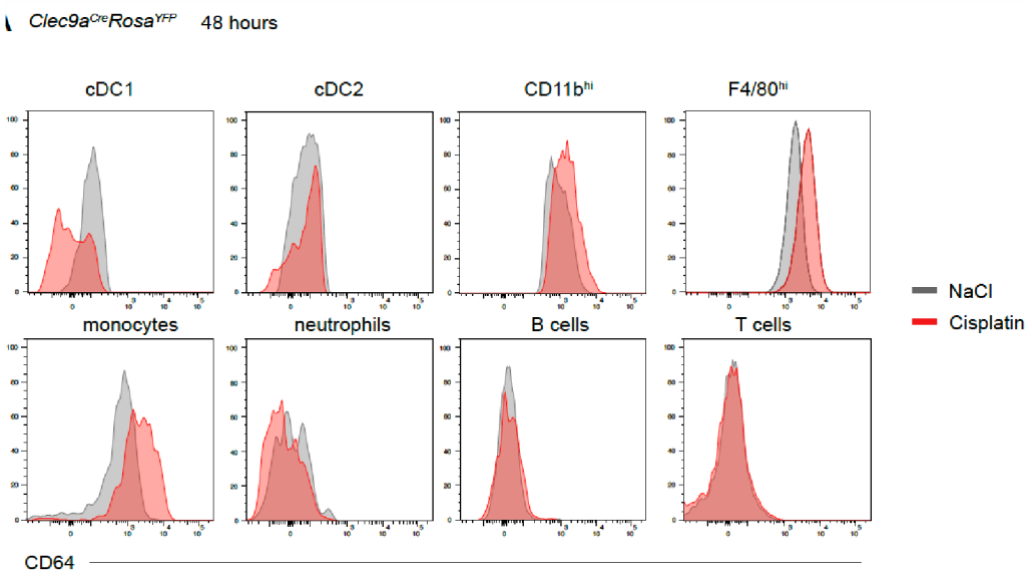

Fig. 13. Cisplatin treatment in Clec9acreRosaYFP mice do not induce CD64 expression on renal immune cell populations which usually do not express it. Clec9a^{cre}Rosa^{YFP} mice were injected with cisplatin for 48 hours, and kidney immune cell populations were analyzed for CD64 expression by flow cytometry. (Modified from Salei et al., 2021)

4.6.5 CD64^{+} MPs depletion in cisplatin induced AKI do not cause neutrophilia

DCs depletion is reported to induce neutrophilia in CD11c-DTR mice (83). To investigate if neutrophilia also happened in Clec9a^{cre}CD64^{iDTR} mice after CD64^{+} MPs depletion, we checked splenocytes to see if neutrophilia happens. Our results showed all of the immune cell populations in the spleen, including neutrophils, do not change in cell counts after renal CD64^{+} MPs depletion in cisplatin induced AKI. Splenic Ly6C^{+} monocytes increased in frequency and T cells decreased in frequency after renal CD64^{+} MPs depletion.

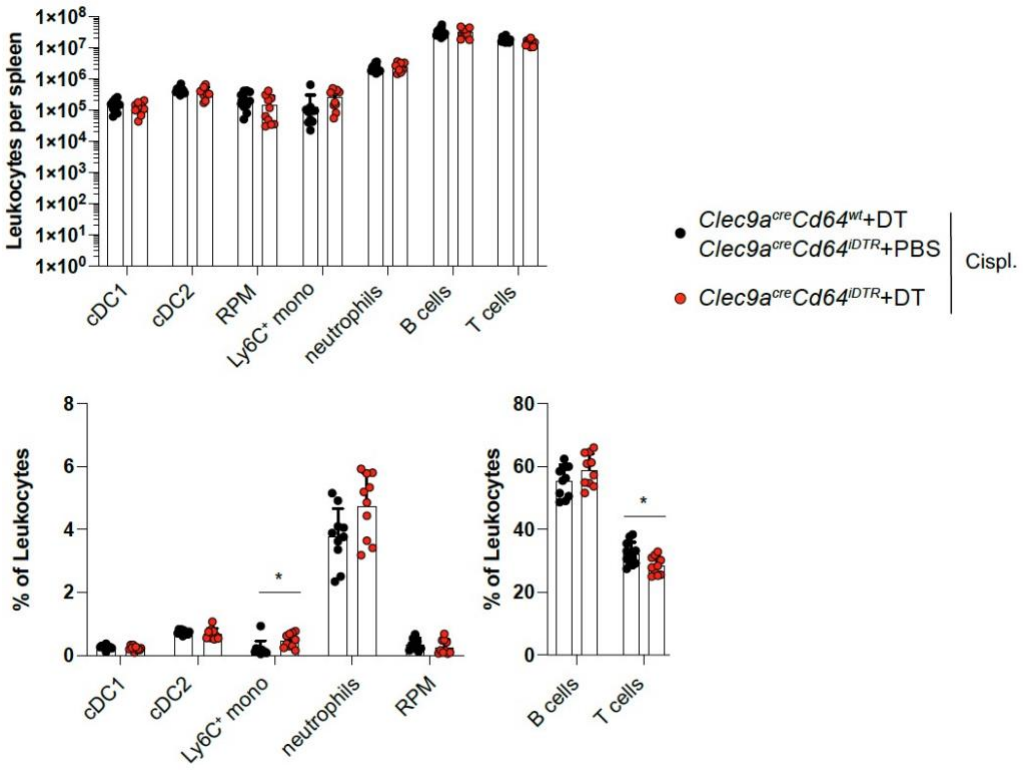

Fig. 14. CD64^{+} MPs depletion does not induce neutrophilia in cisplatin induced AKI. Clec9a^{cre}CD64^{iDTR} mice were i.p. injected with DT to depleted CD64^{+} MPs, control mice were Clec9a^{cre}CD64^{wt} mice i.p. injected with DT, Clec9a^{cre}CD64^{iDTR} mice were injected with PBS. 24 hours later all mice were i.p. injected with cisplatin to induce acute kidney injury. 48 hours later all renal immune cell subsets were analyzed by flow cytometry. Cell counts and frequency were shown as indicated. * $p<0.05$. Student's t test. Data from 2 independent experiments. (Modified from Salei et al., 2021)

4.7 CD64^{+} MPs protect kidney function both in steady state and inflammation

4.7.1 GFR decreased in CD64^{+} MP-depleted mice post IRI for 5 days

To investigate CD64^{+} MPs´ function post IRI for 5 days, we firstly depleted CD64^{+} MPs in Clec9a^{cre}CD64^{iDTR} mice on Day -1 and then induced unilateral IRI injury on Day 0. Unilateral IRI injury was performed by clamping left hilum for 25 min. We checked GFR on Day -3, Day 0 and Day 5 (Fig. 15A). GFR on Day -3 was measured as kidney function baseline, GFR on Day 0 was measured to check if DT injection affects kidney function, GFR on Day 5 was measured to check if CD64^{+} MPs depleted mice have worse kidney function compare with non-depleted mice after IRI. Our data showed that DT injection did not affect kidney function (Fig. 15B). GFR in non-depleted mice did not change significantly on Day 5 compare with Day 0 (Fig.15C Left panel closed circle vs. opened circle), but in CD64^{+} MP-depleted mice GFR decreased very significant on Day 5 compare with Day 0 (Fig.15C Left panel closed triangle vs. opened triangle), indicating CD64^{+} MPs protect kidney function. Body weight (B.W) in CD64^{+} MP-depleted mice dropped very significantly on Day 5 compare with Day 0 (Fig.15C Right panel closed triangle vs. opened triangle), but this not happened in non-depleted mice (Fig.15C Right panel closed circle vs. opened circle), indicating CD64^{+} MPs also maintain normal body weight in IRI (Fig. 15C). We also checked blood urea nitrogen (BUN) and serum creatinine, they did not change due to functional compensation of contralateral kidney (Fig. 15D).

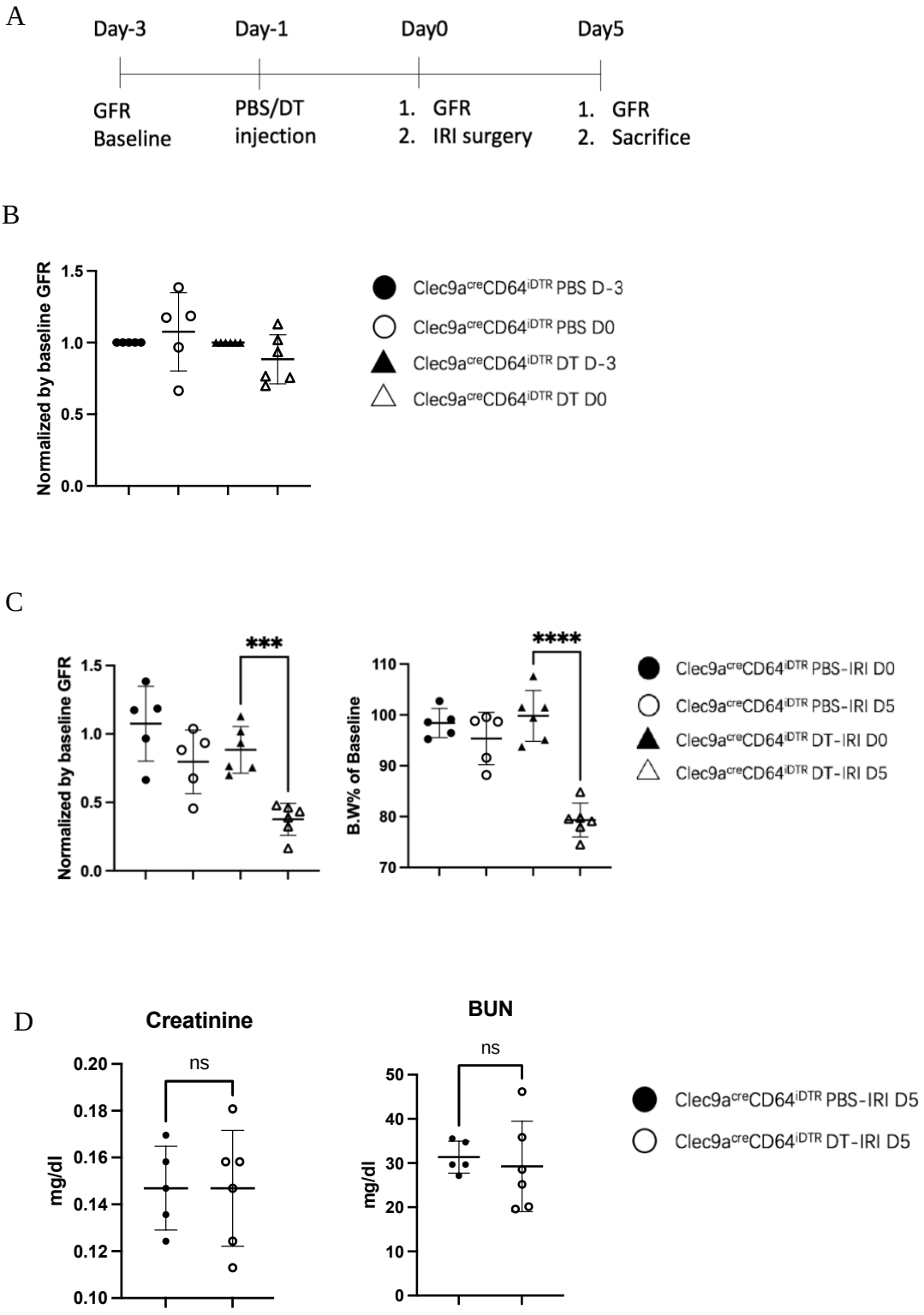

Fig. 15. CD64^{+} MPs depletion leads to more severe injury post IRI surgery for 5 days. Clec9a^{cre}CD64^{iDTR} mice is measured of GFR on Day -3 as baseline, on Day -1 mice are i.p. injected with PBS or DT, on Day 0 GFR is checked and then all mice are performed with unilateral IRI surgery by clamping the left kidney pedicle for 25min, on Day 5 GFR is measured and then all mice are sacrificed. (A) Scheme of experiment design. (B) Day -3

and Day 0 GFR from Clec9a^{cre}CD64^{iDTR} mice injected with PBS or DT. (C) Day 0 and 5 GFR from Clec9a^{cre}CD64^{iDTR} mice i.p. injected with PBS or DT and performed unilateral IRI surgery and B.W on Day 0 and Day 5 are indicated. (D) BUN and serum creatinine are indicated. Each dot represents one mouse. One-way ANOVA was used for analysis (B and C), horizontal bars represent mean, error bars represent SD, *p<0.05, ** p<0.01, *** p<0.005, ****p<0.001, only significant differences are indicated. Student's t test was used for analysis (D), ns means not significant. Data from 2 independent experiments.

4.7.2 Renal cDC1, cDC2, Ly6c+, monocytes, neutrophils and T cells decreased significantly in IRI operated kidneys after CD64$^+$ MPs depletion post IRI for 5 days

To investigate which immune subsets contribute to deteriorated kidney injury after CD64$^+$ MPs depletion post IRI for 5 days, we used flow cytometry to profile each population in the kidney. Our results showed F4/80^{hi} cells kept depleted in contralateral and IRI operated kidneys in DT injected mice post IRI for 5 days, cDC1, cDC2, monocytes, neutrophils, Ly6c+ and T cells in IRI operated kidneys were also decreased, it is possible CD64$^+$ MPs can activate cDC1/cDC2 mediated T cell proliferation, and this effect is abrogated once CD64$^+$ MPs are depleted in IRI. Monocytes, neutrophils and Ly6C$^+$ cells were decreased only in IRI side kidney after CD64$^+$ MPs depletion, indicating infiltration into injured kidney is weaken. MHCII$^-$F4/80^{hi} cells upregulated in IRI operated kidneys is due to down-regulation of MHCII expressed on F4/80^{hi} cells in inflammation (49, 63). B cells did not have significant change after CD64$^+$ MPs depletion post IRI for 5 days. Frequencies of F4/80^{hi}, CD11b^{hi}, cDC2, B cells, monocytes and T cells did not show significant decrease if comparing non-depleted and depleted mice in both the contralateral kidneys and IRI operated kidney. cDC1 frequency decreased in contralateral kidneys.

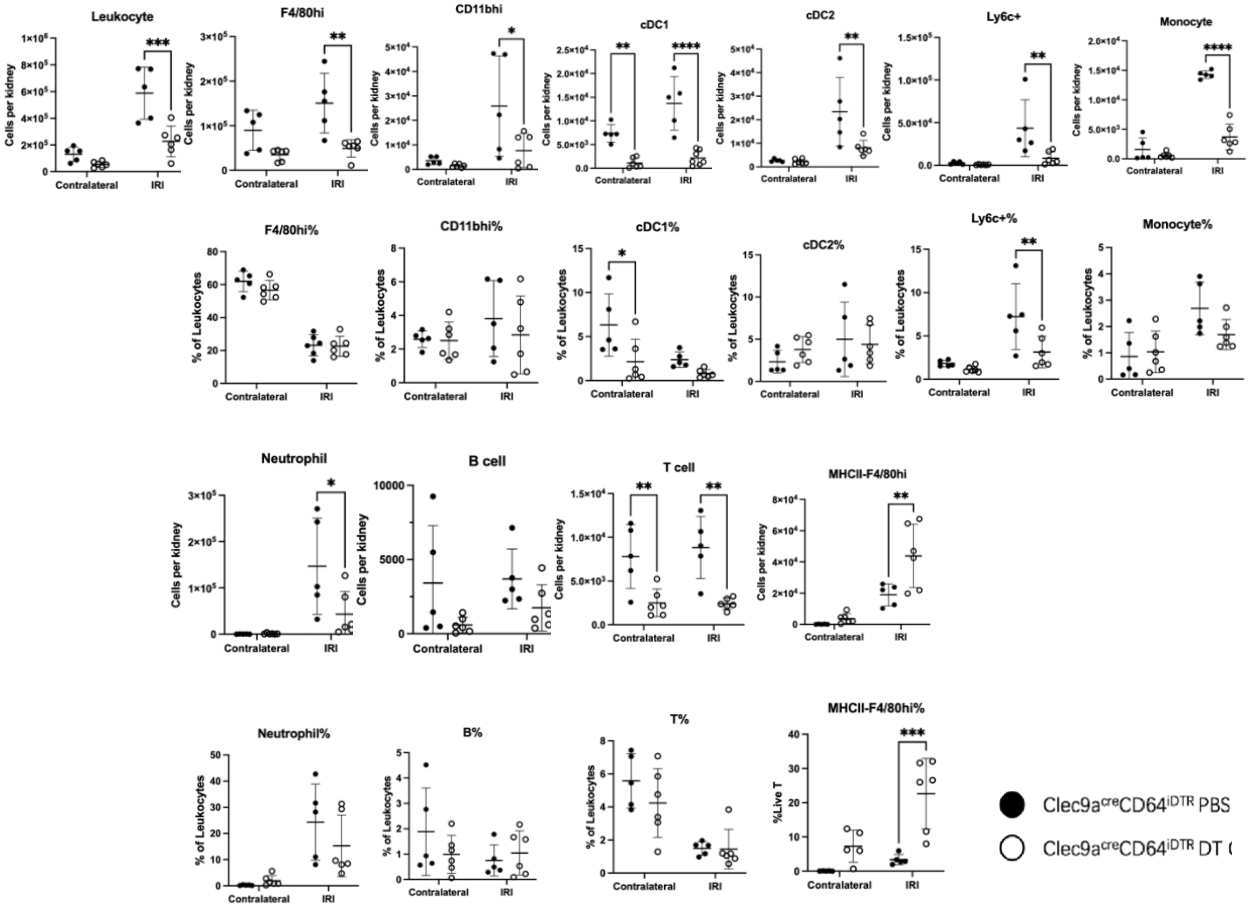

Fig. 16. Renal cDC1, cDC2, Ly6c+, monocytes, neutrophils and T cells decreased significantly in IRI operated kidneys after CD64+ MPs depletion post IRI for 5 days. Clec9a^{cre}CD64^{iDTR} mice are measured of GFR on Day -3 as baseline, on Day -1 mice are i.p. injected with PBS or DT, on Day 5 all mice are measured with GFR and then sacrificed. Two-way ANOVA was used for analysis, * $p<0.05$, ** $p<0.01$, *** $p<0.001$, **** $p<0.0001$, only significant differences are indicated. Data from 2 independent experiments.

4.7.3 CD8$^+$ T cell, Th1, Th17 and Treg decreased after CD64$^+$ MPs depletion in both contralateral and IRI operated kidneys post IRI for 5 days but not significant

T cells contain multiple subsets, they are classified as CD3$^+$CD4$^+$ T helper cells and CD3$^+$CD8$^+$ cytotoxic T cells. T helper cells can be further subdivided into Th1, Th2, Th17 and T regulatory cells (Treg). Th1 cells can produce interferon γ (IFN- γ), Th2 cells can produce IL-4, Th17 cells produce IL-17 and Treg can suppress proinflammatory cytokine production by other cells (84). It is reported T cells promote kidney injury by various

mechanisms such as FasL expressed on T cells combined with Fas on tubular epithelial cells to induce apoptosis (85). In cisplatin induced AKI, $CD4^+$ T cells can produce CXCL1 to recruit neutrophils to injured kidney (86). Since we saw total T cells decreased significantly in both contralateral and IRI operated kidneys after $CD64^+$ MPs depletion post IRI for 5 days, we are wondering which T cell subsets decreased mostly that led to the total T cells loss. We isolated total leukocytes in both $CD64^+$ MPs non-depleted and depleted mice and stained them by intracellular T cell subsets panel and then used flow cytometry to analyze the T cell subsets. We used CD8, IFN- γ, TNFa, IL-17 and Foxp3 to identify $CD8^+$ T cell, Th1, Th17 and Treg respectively (Fig. 17A). Our results showed that all of these T cell subsets decreased both in contralateral and IRI operated kidneys after $CD64^+$ MPs depletion post IRI for 5 days, although not statistically significant, the trend is obvious (Fig. 17B), it may indicate T cell loss is due to abrogated interaction between $CD64^+$ MPs and T cells.

A

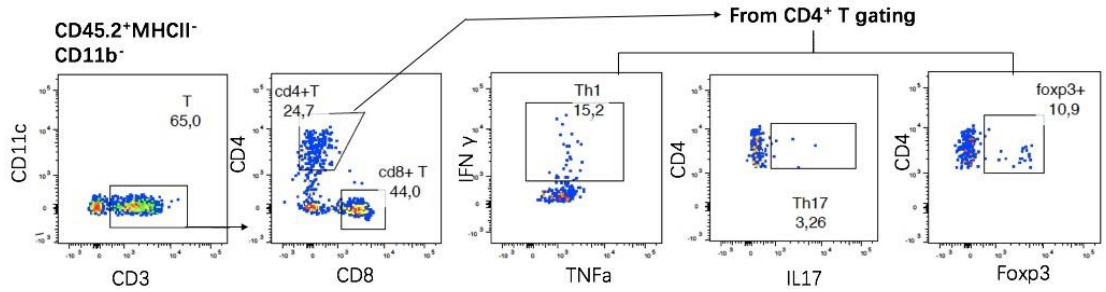

B

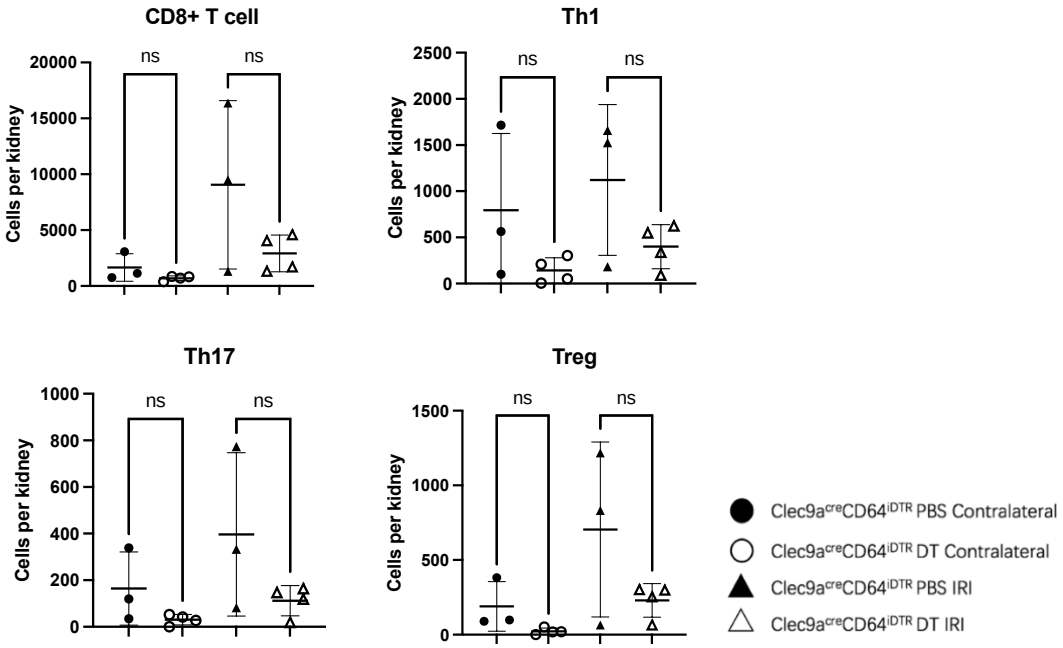

Fig. 17. CD8$^+$ T cell, Th1, Th17 and Treg decreased but not significant after CD64$^+$ MPs depletion post IRI for 5 days. Clec9a^{cre}CD64^{iDTR} mice are measured of GFR on Day -3 as baseline, on Day -1 mice are injected with PBS or DT, on Day 5 all mice are measured with GFR and then sacrificed for T cell intracellular staining, CD8$^+$ T cell, Th1, Th17 and Treg are identified as CD8$^+$ cells, IFN- γ^+TNFa$^+$ cells, IL-17$^+$ cells and Foxp3$^+$ cells respectively. (A) Representative gating of T cell subsets. (B) Quantification of T cell subsets. Two-way ANOVA was used for analysis (B), ns means not significant. Data from 1 experiment.

4.7.4 cDC1 depletion in XCR1-venus-DTR mice post IRI for 3 days does not affect AKI severity

Since in 4.7.1 we found $CD64^+$ MPs depletion deteriorated kidney injury severity post IRI for 5 days, and at this time point we saw cDC1 is decreased, we are curious if cDC1 depletion alone will affect kidney injury severity. To answer this question, we injected DT in XCR1-venus-DTR mice to deplete cDC1 on Day -1, on Day 0 we performed unilateral IRI surgery, on Day 3 we checked GFR (Fig.18 A). Our result showed that: 1) DT injection did not affect kidney function by measuring GFR (Fig.18 B), and 2) cDC1 depletion did not affect kidney injury severity post IRI for 3 days (Fig.18 B). By checking cell numbers, we found cDC1 were depleted significantly and specifically in contralateral kidneys, while $Ly6C^+$ cell numbers reduced in IRI operated kidney on Day 3 but other populations did not change (Fig.18 C). We also checked blood urea nitrogen (BUN) and serum creatinine level after cDC1 depletion post IRI operation for 4 days, we did not see significant change (Fig.18 D). In conclusion, cDC1 depletion alone did not affect IRI injury post IRI for 3 days, and it is unlikely the direct reason for kidney function loses in $CD64^+$ MPs depleted mice post IRI for 5 days in 4.7.1 since the window for GFR measurement is similar.

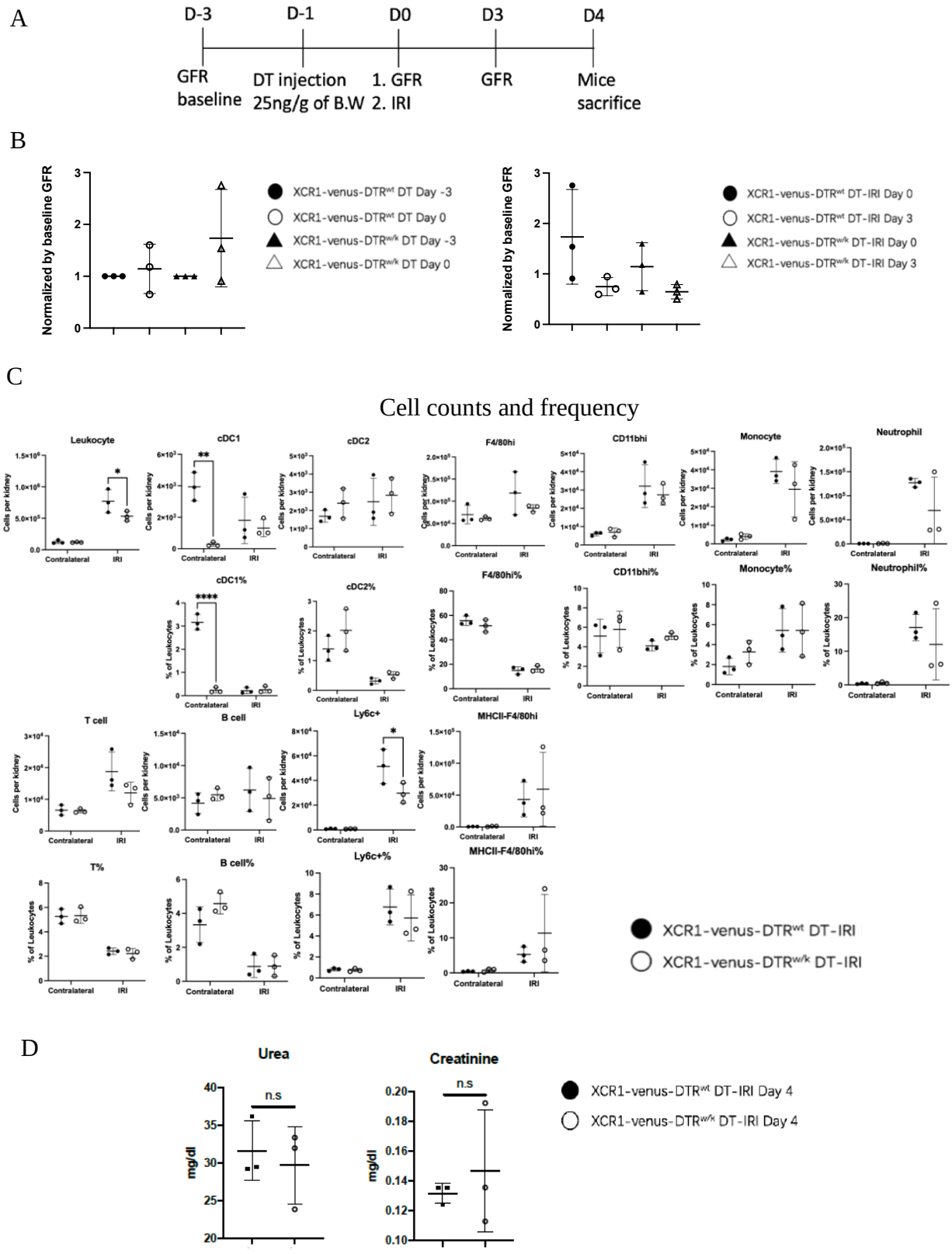

Fig. 18. cDC1 depletion does not affect kidney injury severity post IRI for 3 days. XCR1-venus-DTR$^{w/w}$ and XCR1-venus-DTR$^{w/k}$ mice are injected with DT, 1 day later all

the mice are performed unilateral IRI by clamping left kidney pedicle for 25min, 3 days later mice are measured for GFR, on Day 4 all mice are sacrificed. (A) Experimental scheme is indicated. (B) Day -3 and Day 0 GFR, Day 0 and Day 3 GFR are indicated. (C) Immune cell subsets counts, and frequencies are indicated. (D) BUN and creatinine are indicated. One-way ANOVA was used for analysis (B), Two-way ANOVA was used for analysis (C), *p<0.05, **p<0.01, ***p<0.005, ****p<0.001, only significant differences are shown. Student's t test was used for analysis (D), n.s means not significant. Data from 1 experiment.

4.7.5 CD64+ MPs depletion 5 days after sham surgery leads to loss of kidney function

Since we saw very significant decrease of GFR in $CD64^+$ MPs depleted mice 5 days after IRI surgery, we are curious if it is caused by $CD64^+$ MPs depletion alone or depletion combined with IRI. To answer this question, we injected PBS/DT in $Clec9a^{cre}CD64^{iDTR}$ mice on Day -1, then we performed unilateral sham surgery on all of these mice on Day 0, 5 days later we measured GFR (Fig. 19A). Our results showed that in C57BL/6JRccHsd mice injected with DT did not have significant change in GFR on Day 0 compare with Day -3, meaning DT injection will not influence kidney function (Fig. 19B). Non-depleted mice did not change in GFR on Day 5 compare with Day 0, but in depleted mice GFR decreased significantly on Day 5 compare with Day 0, indicating depletion of this population will lead to loss of kidney function even without IRI surgery (Fig. 19C). By comparing body weight on Day 0 and Day 5, we found body weight dropped significantly in $CD64^+$ MPs depleted mice (Fig. 19D). We also checked blood urea nitrogen (BUN) and serum creatinine level after $CD64^+$ MPs depletion post Sham operation for 5 days, we did not see significant decrease in depleted mice on Day 5 compare with Day 0 due to the compensation of contralateral kidney (Fig. 19E). In conclusion, $CD64^+$ MPs maintain kidney function in steady state, and depletion of this population for 5 days will lead to loss of kidney function.

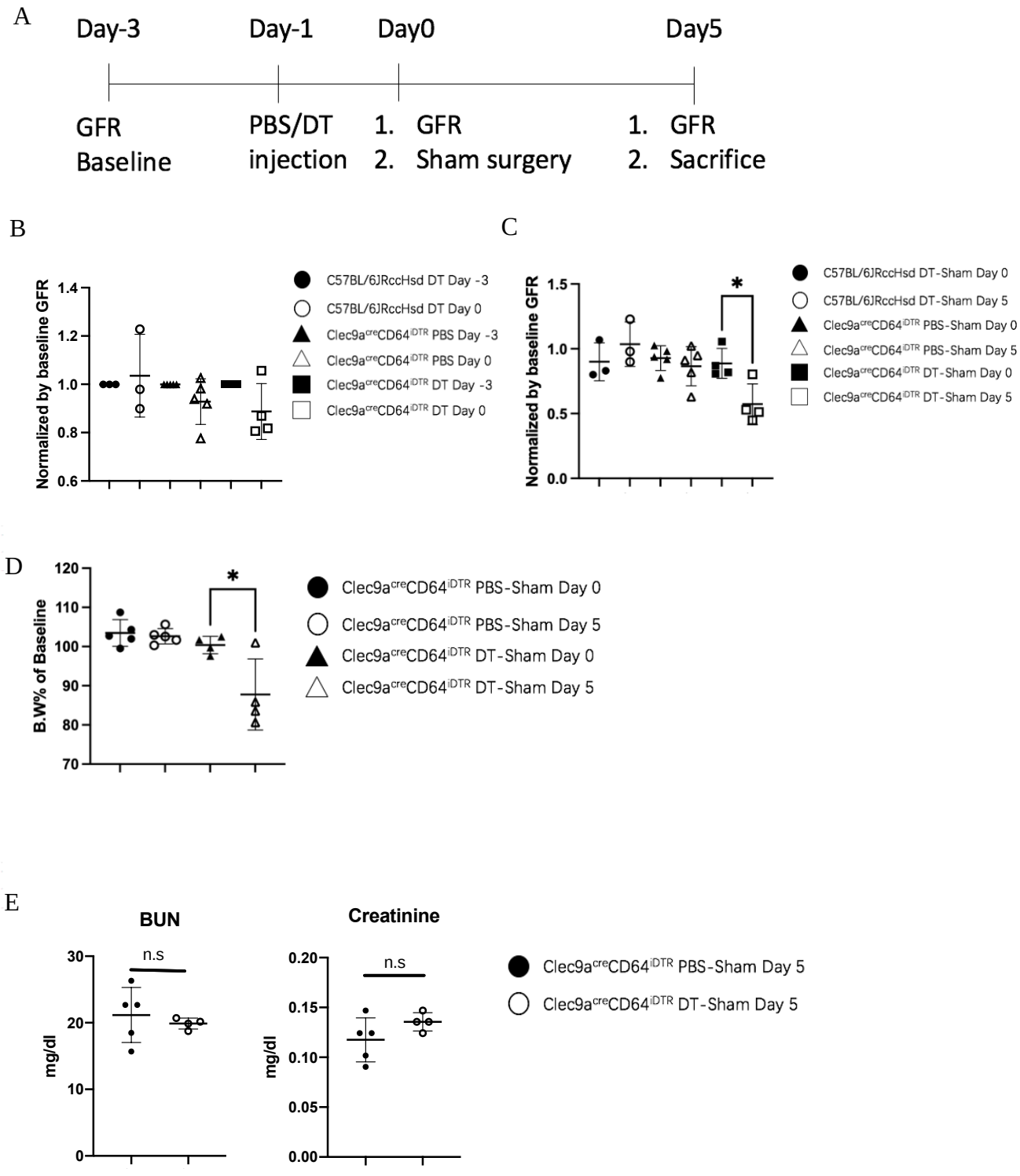

Fig. 19. CD64^{+} MPs depletion leads to loss of kidney function in mice 5 days after sham surgery. C56BL/6JRccHsd and Clec9a^{cre}CD64^{iDTR} mice were measured of GFR on Day -3 as baseline, on Day -1 C57BL/6JRccHsd mice are injected with DT, and Clec9a^{cre}CD64^{iDTR} mice are i.p. injected with PBS or DT, on Day 0 GFR is measured and then all mice are performed with unilateral sham surgery, on Day 5 GFR is measured and

then all mice are sacrificed. (A) Scheme of experiment design. (B) Day -3 and 0 GFR from C57BL/6JRccHsd mice i.p. injected with DT and Clec9a^{cre}CD64^{iDTR} mice injected with PBS or DT. (C) Day 0 and 5 GFR from C57BL/6JRccHsd mice injected with DT and Clec9a^{cre}CD64^{iDTR} mice injected with PBS or DT and performed unilateral sham surgery. (D) Body weight loss of all mice are indicated. (E) BUN and creatinine are indicated. Each dot represents one mouse. One-way ANOVA was used for analysis (B, C and D), * $p<0.05$, ** $p<0.01$, only significant differences are shown. Student's t test was used for analysis (E), n.s means not significant. Data from 2 independent experiments.

4.7.6 Renal B cells and T cells were decreased in CD64+ MPs depleted mice 5 days after sham surgery

To investigate which immune cell subsets contributed to decreased GFR in CD64^{+} MPs 5 days after sham surgery, we used flow cytometry to profile the immune cell populations in kidney, our results showed that CD64^{+} MPs and CD11b^{hi} cells kept depleted on Day 5, we also found B cells and T cells decreased significantly on Day 5 in CD64^{+} MP depleted mice compare with non-depleted mice in contralateral kidneys. cDC1, cDC2, neutrophils, monocytes, Ly6C^{+} cells and MHCII^{-}F4/80^{hi} cell counts do not change significantly in CD64^{+} MP-depleted mice compare with non-depleted mice, but MHCII^{-}F4/80^{hi} frequency increased in CD64^{+} MP-depleted mice sham kidneys. In conclusion, increased kidney injury severity in CD64^{+} MP-depleted mice 5 days after sham surgery may be attributed to loss of CD64^{+} MPs, CD11b^{hi} cells, B cells and T cells.

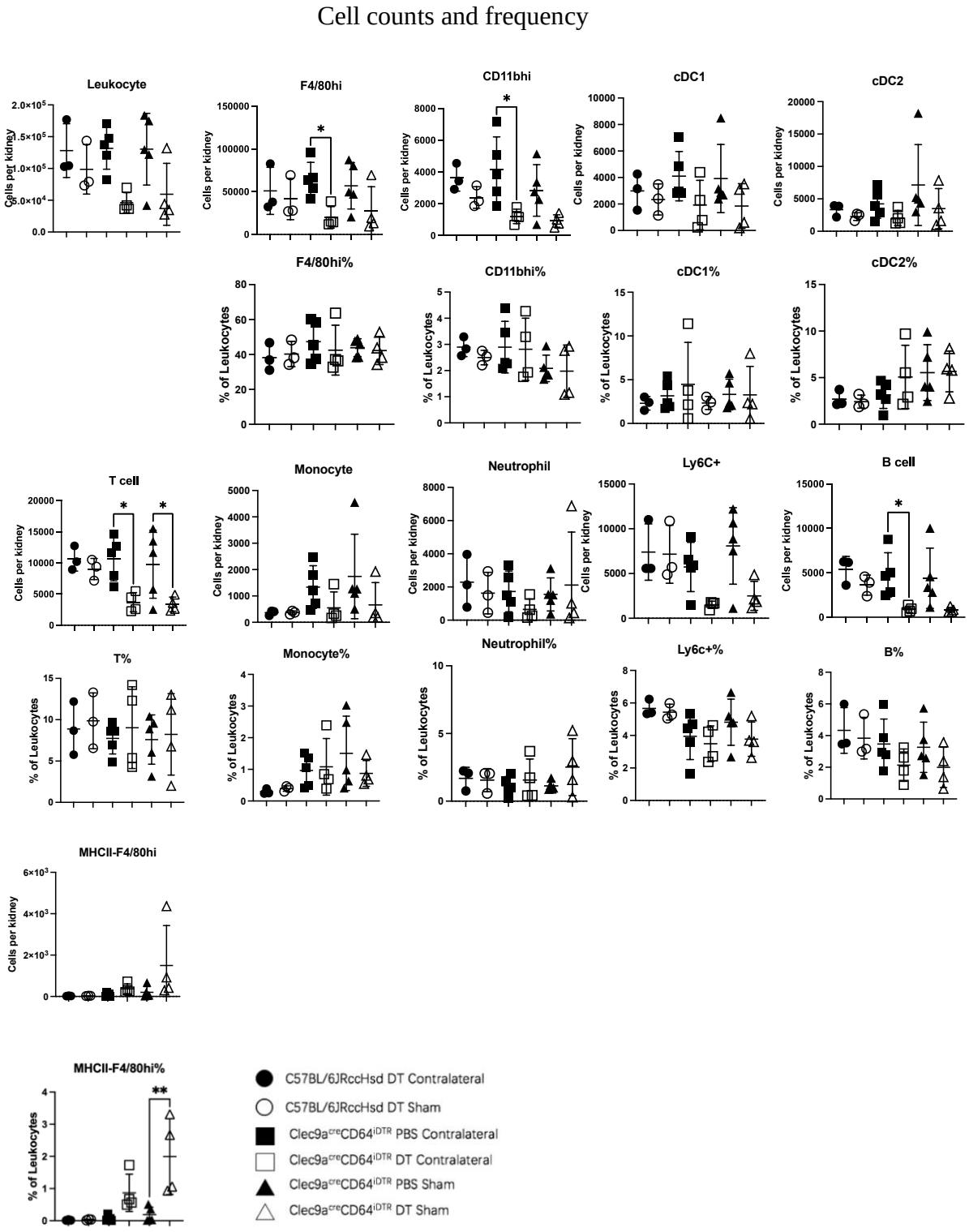

Fig. 20. Renal B cells and T cells decreased in CD64+ MPs depleted mice 5 days after sham surgery. C56BL/6JRccHsd mice are injected with DT, Clec9a^{cre}CD64^{iDTR} mice are injected with PBS or DT on Day -1, on Day 5 all mice are sacrificed, and kidneys are taken for flow cytometry analysis. Immune subsets cell counts, and frequencies are indicated.

Two-way ANOVA was used for analysis. * p<0.05, ** p<0.01, *** p<0.005, only significant differences are shown. Data from 2 independent experiments.

4.7.7 CD64+ MPs depletion does not lead to neutrophilia in spleen 5 days after sham surgery

Dendritic cell depletion in CD11c-DTR model will lead to neutrophilia (87), we are wondering if $CD64^+$ MP-depletion in $Clec9a^{cre}CD64^{iDTR}$ model will also lead to neutrophilia which could be the cause of decreased GFR in sham operated mice. To answer this question, we used flow cytometry to check splenic neutrophils in $CD64^+$ MP-depleted mice 5 days after sham surgery. Our results showed after $CD64^+$ MP- depletion, we did not see neutrophilia in spleen, indicating decreased GFR is not caused by neutrophilia.

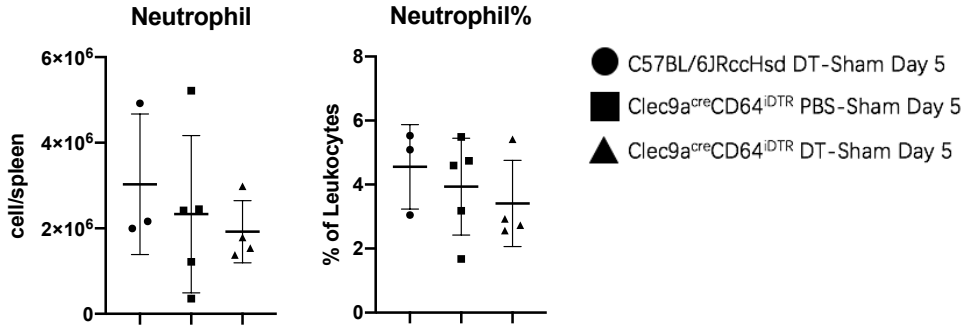

Fig. 21. CD64+ MP-depletion 5 days after sham surgery does not induce neutrophilia. C56BL/6JRccHsd mice are injected with DT and $Clec9a^{cre}CD64^{iDTR}$ mice are injected with PBS or DT on Day -1, on Day 5 all mice are sacrificed, and spleens are taken for flow cytometry analysis. Neutrophil cell counts and frequency are indicated. One-way ANOVA was used for analysis. Data from 2 independent experiments.

4.7.8 GFR does not change in CD64+ MP-depleted mice 24 hours after sham surgery

Since depletion of $CD64^+$ MPs will lead to decreased GFR 5 days after sham surgery, we are curious if kidney function will also be influenced 24 hours after sham surgery. Our result showed that GFR does not change in $Clec9a^{cre}CD64^{iDTR}$ mice depleted of $CD64^+$ MPs, indicating at this time point the depletion of $CD64^+$ MPs has not caused function loss to the kidney, and it is a good timing for investigating $CD64^+$ MPs function in acute phase

of IRI (Fig. 22A). By checking body weight, we found it does not have significant difference in CD64^{+} MP-depleted mice on Day 1 (Fig. 22B).

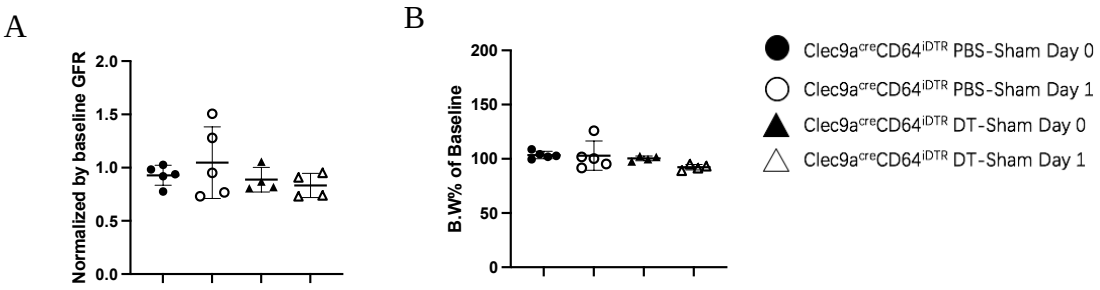

Fig. 22. CD64^{+} MP-depletion 24 hours after sham surgery does not affect GFR. Clec9a^{cre}CD64^{iDTR} mice are measured of GFR on Day -3 as baseline, on Day -1 all mice are injected with i.p. PBS or DT, on Day 0 GFR is measured and then all mice are performed with unilateral sham surgery, on Day 1 GFR is measured. (A) GFR of all mice both from Day 0 and Day 1 are indicated. (B) Body weight loss of all mice are indicated. One-way ANOVA was used for analysis. Data from 2 independent experiments.

4.7.9 CD64^{+} MP-depletion does not affect injury severity 24 hours after IRI surgery compare with non-depleted mice

Since we confirmed CD64^{+} MP-depletion 24 hours after sham surgery does not induce decreased GFR, we decided to induce IRI injury at this time point. We firstly depleted CD64^{+} MPs on Day -1, on Day 0 we performed unilateral IRI operation to induced AKI, on Day 1 we measured GFR (Fig.23A). Our results showed that IRI surgery successfully induced injury both in Clec9a^{cre}CD64^{iDTR} mice injected with PBS and DT on Day 1 since GFR decreased very significantly compare with Day 0 (Fig.23B). However, by comparing Clec9a^{cre}CD64^{iDTR} mice treated with PBS-IRI and DT-IRI, we found the GFR does not have significant difference in CD64^{+} MP-depleted mice compare with non-depleted mice on Day 1 (Fig.23B Open circles vs. open triangles), meaning CD64^{+} MPs could not show their protective effect at this time point. We also checked BUN (blood urea nitrogen) and creatinine level (Fig. 23C), they did not change significantly due to contralateral kidney compensated the function loss of IRI operated kidney.

A

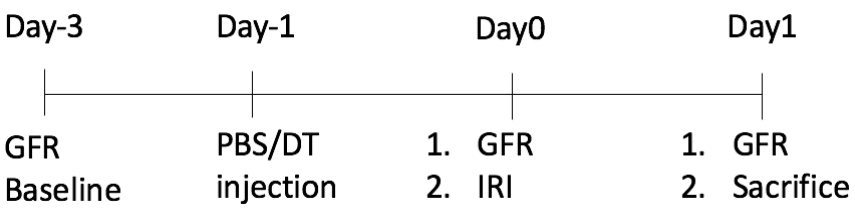

B

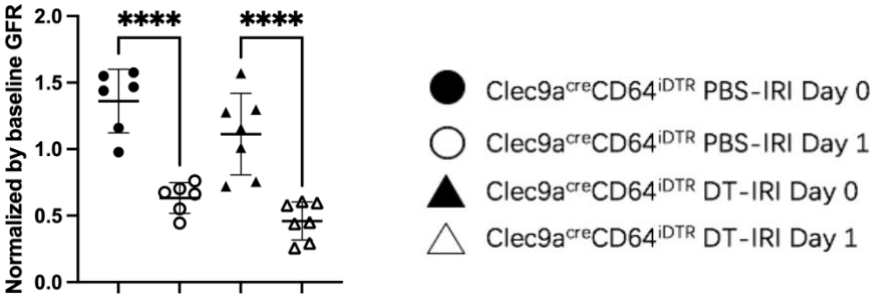

C

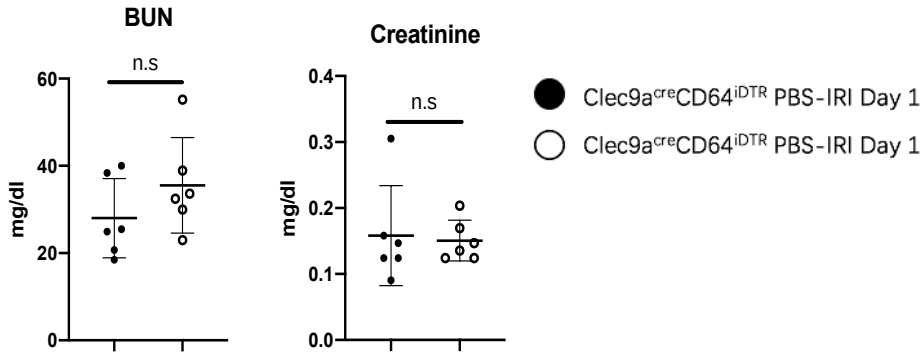

Fig. 23. GFR does not decrease in mice depleted of CD64+ MPs 24 hours after IRI surgery. Clec9a^{cre}CD64^{iDTR} mice are measured of GFR on Day -3 as baseline, on Day -1 Clec9a^{cre}CD64^{iDTR} mice are i.p. injected with PBS or DT, on Day 0 GFR is measured and then all mice are performed with unilateral IRI surgery, on Day 1 GFR is measured. (A) Experimental design. (B) GFR of all mice both from Day 0 and Day 1 are indicated. One-way ANOVA was used for analysis (B), each dot represents one mouse, horizontal bars represent mean, error bars represent SD, only significant differences are indicated, **p<0.01, ****p<0.001. Student's t test was used for analysis (C), horizontal bars represent

mean, error bars represent SD, n.s means not significant. Data are combined from two independent experiments.

4.7.10 CD64+ MPs kept depleted in contralateral kidney post IRI surgery for 24 hours

We found not significant difference in GFR from non-depleted and depleted mice 24 hours post IRI surgery, indicating cell depletion has no effect on injury during the inflammation phase. But taking into consideration that GFR was reduced significantly in depleted mice on Day 5 post IRI, it is meaningful to profile renal immune subsets to confirm if there are populations have significant changes in depleted mice which may potentially lead to reduced GFR on Day 5. We used flow cytometry to check all immune subsets in both contralateral and IRI operated kidneys. Our results show F4/80^{hi} cells are depleted in contralateral kidney, monocytes and Ly6C^{+} cells are increased in frequency in contralateral kidney due to reduced leukocytes as normalization factor, other subsets do not change significantly. This data indicates the exacerbated injury on Day 5 is possibly due to loss of CD64^{+} MPs.

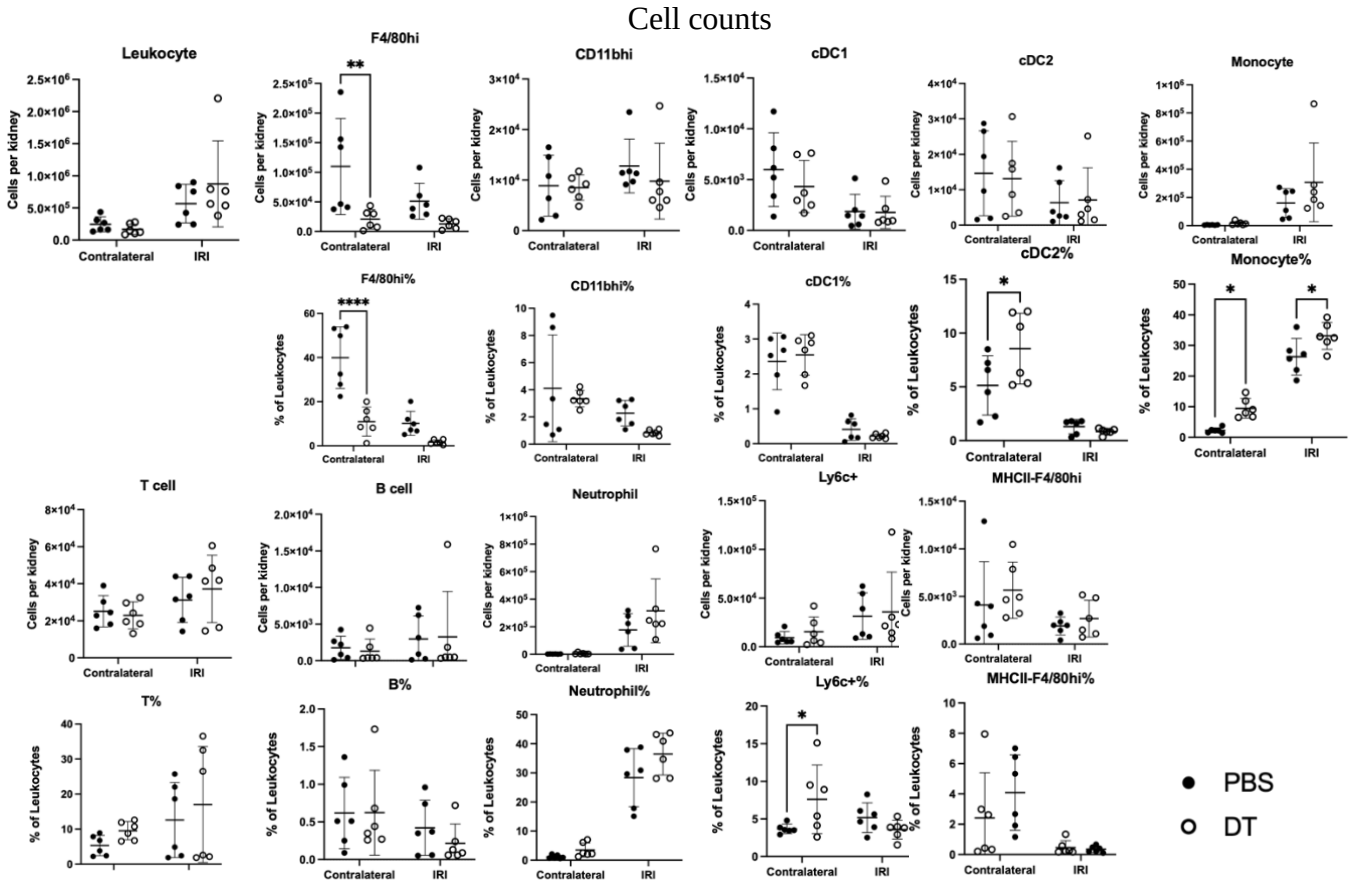

Fig. 24. CD64^{+} MPs kept depleted in contralateral kidney 24 hours after IRI surgery. Clec9a^{cre}CD64^{iDTR} mice are injected with PBS or DT on Day -1, on Day 1 all mice are sacrificed, and kidneys are taken for flow cytometry analysis. Immune subsets counts and frequency are indicated. Two-way ANOVA was used for analysis, * $p<0.05$, ** $p<0.01$, **** $p<0.0001$, only significant differences are shown. Data from 2 independent experiments.

4.7.11 IL-6, IL-18, TNF-α and TGF-β do not change after CD64^{+} MP-depletion 24 hours after IRI surgery

Since CD64^{+} MPs are depleted in contralateral kidney and also decreased in IRI operated kidneys, considering they can produce cytokines to mediate immune response in inflammation, so we checked cytokines by qPCR from total tissue mRNA. IL-6 is reported correlating with onset and severity of AKI (88), our result showed that IL-6 does not change significantly in IRI kidney after CD64^{+} MP-depletion (Fig. 25). IL-18 is reported deteriorating kidney damage in IRI AKI (89), and IL-18 full knock out ameliorates kidney

tubular cells damage and reduced neutrophil infiltration, by checking IL-18 mRNA level, we found IL-18 does not alter significantly in IRI kidney in $CD64^+$ MP- depleted mice (Fig. 25). TNF-α is reported upregulated during tubular cell apoptosis (90), we checked TNF-a expression and found it does not have significant change after $CD64^+$ MP-depletion in IRI kidney (Fig. 25). TGF-β signaling is another pathway that been reported activated by IRI, we checked TGF-β mRNA and found it does not have significant alteration after $CD64^+$ MP-depletion in IRI operated kidney (Fig. 25). In conclusion, IL-6, IL-18, TNF-α and TGF-β are not found changed dramatically in $CD64^+$ MP-depleted mice IRI operated kidneys, it could be attributed to the reason that these inflammatory cytokines may not play very important role in this case, or due to other reason such as the cytokines mRNA is diluted out by kidney tissue cell mRNA so that cytokines produced by immune cells cannot be detected.

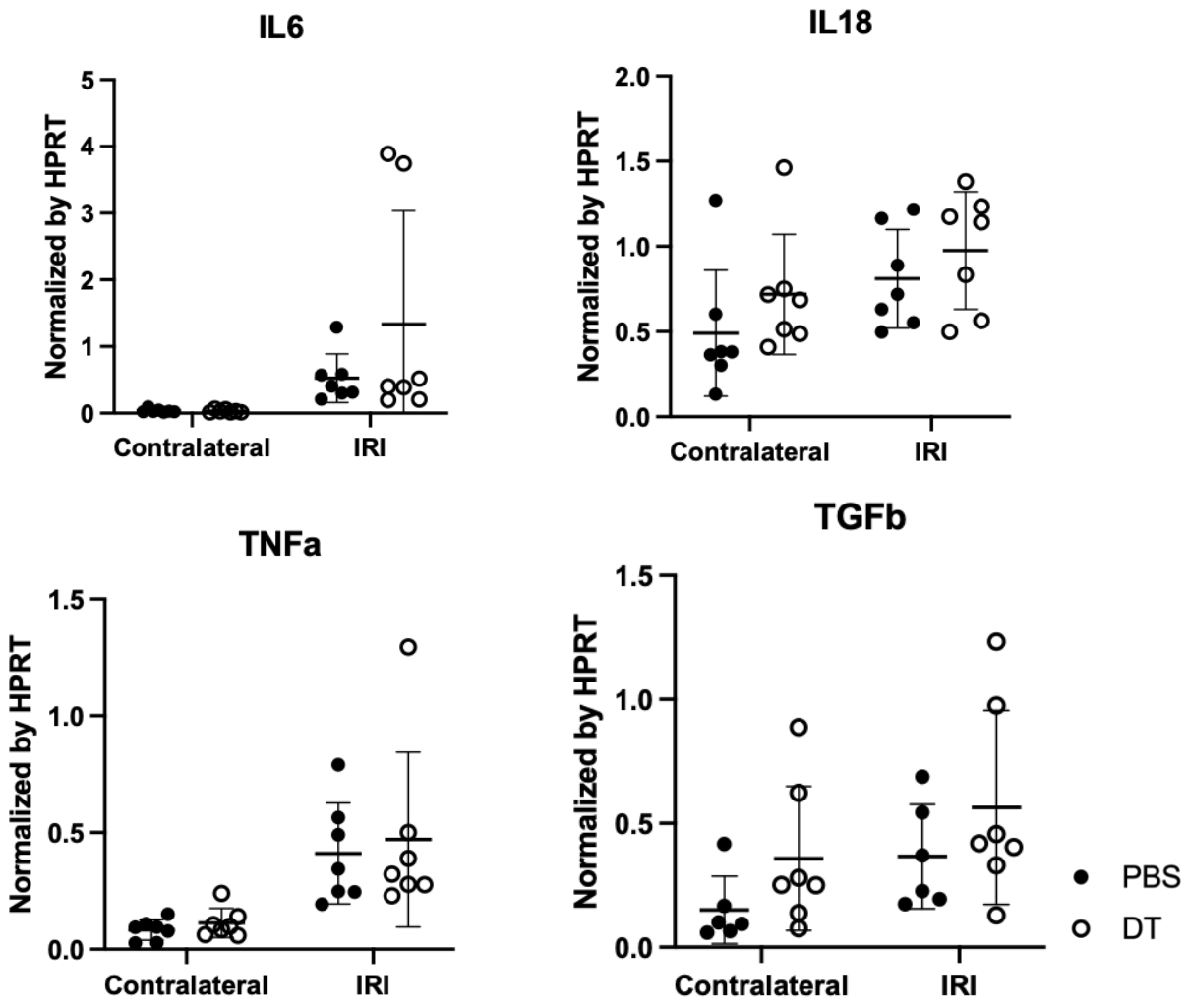

Fig. 25. IL-6, IL-18, TNF-α and TGF-β expression do not change in CD64^{+} MP-depleted mice 24 hours after IRI surgery. Clec9a^{cre}CD64^{iDTR} mice are i.p. injected with PBS or DT, 1 day later all the mice are performed unilateral kidney IRI by clamping left kidney pedicle for 25min, 1 day later all mice are sacrificed for qPCR analysis. IL-6, IL-18, TNF-α and TGF-β mRNA levels are indicated. Two-way ANOVA was used for analysis. Only significant differences will be shown. Data from 2 independent experiments.

4.7.12 IFN-β increased significantly in culture supernatant after F4/80hi cells stimulated with histone

In AKI, dying tubular epithelia cells release histone into extracellular space, which interact with TLR2 and TLR4 on immune cells to induce inflammatory signaling activation such as MyD88 and NF-kB pathway (91). Since bulk cytokine qPCR test can only check universal tissue mRNA alteration, in order to check cytokines specifically produced by CD64^{+} MPs, we used histone to stimulate sorted F4/80^{hi} cells in vitro overnight, then we used beads assay kit Legendplex to detect various cytokines in the collected culture supernatant. It is reported BMDC (Bone marrow derived dendritic cell) can produce TNF-α and IL-6 induced by histone (91), so we used mouse BMDC as positive control for measuring cytokine production by F4/80^{hi} cells. Zymosan is reported to induce TNF-α and IL-12p40 production in F4/80^{hi} cells (63), so we used zymosan to stimulate F4/80^{hi} cells as positive control for histone stimulated F4/80^{hi} cells. We stimulated both sorted BMDC and F4/80^{hi} cells with zymosan (10ug/ml) or histone (50ug/ml) for 16 hours, then we collected supernatant for cytokine beads assay. Our results showed that IFN-β increased significantly in histone treated F4/80^{hi} cells compare with F4/80^{hi} cells without treatment (Fig.26 IFN-β Open circles vs. Open triangle). TNF-α, IL-1β, MCP-1, IL-1α do not have significant change. IL-6 increased in zymosan treated cells due to TLR signaling activation as expected, but not in histone treated cells compare with cells without treatment (Fig.26 IL-6 Open circles vs. Open square).

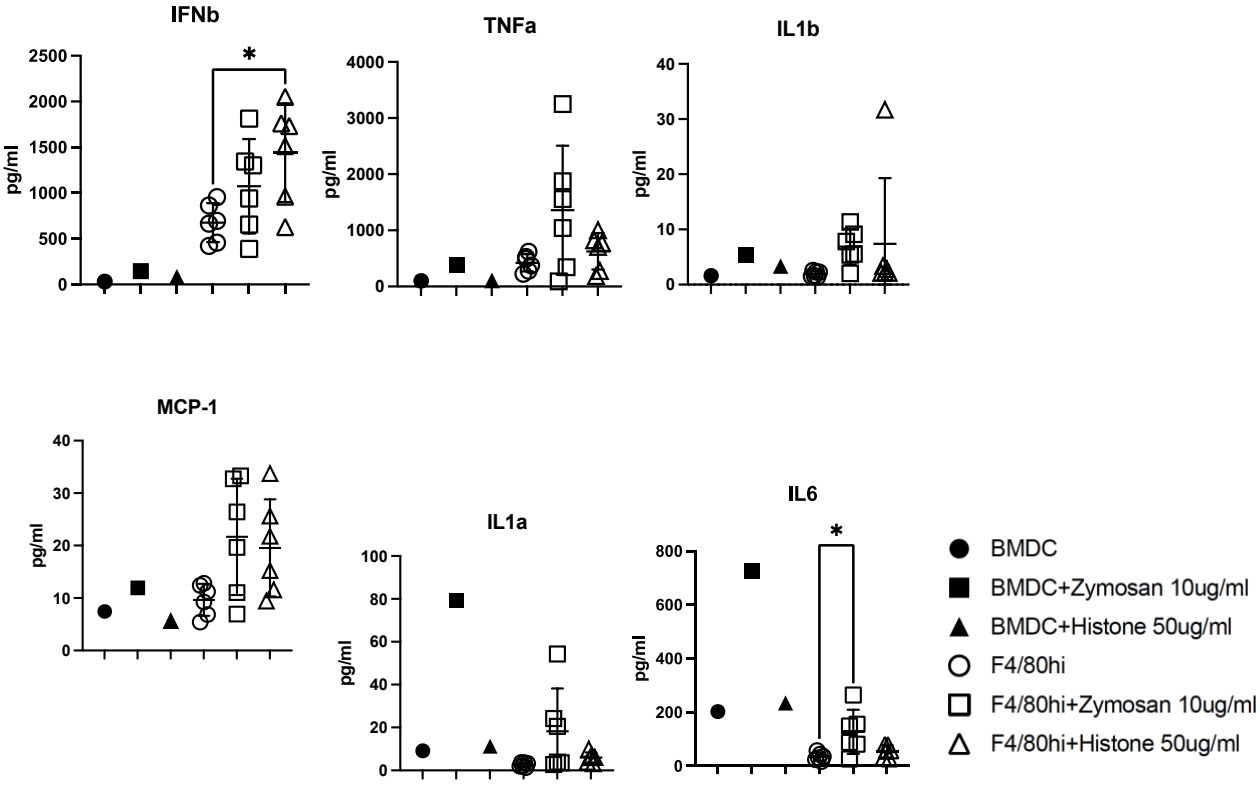

Fig. 26. IFN-β increased F4/80hi cells culture supernatant after histone stimulation for 16 hours. Sorted mouse BMDC and F4/80^{hi} cells are seeded in U-bottom plate (10,000 cells/well) and stimulated with zymosan (10ug/ml) and histone (50ug/ml) for 16 hours, then supernatant is collected for Legendplex beads assay. IL-1α, IFN-β, MCP1, IL-1β, IL-6 and TNF-α are indicated. One-way ANOVA was used for analysis. Only significant differences are indicated. *$p<0.05$, n=6, error bars represent SD. Data from 1 experiment.

Discussion

1. Clec9a^{cre}CD64^{iDTR} mice are a powerful model to study CD64+ MPs function in cisplatin induced AKI

Due to the marker overlapping of renal MPs, it is hard to distinguish different subtypes from each other. In kidney there exist at 4 subsets of MPs which have Clec9a expression history.

Clec9a^{cre}CD64^{iDTR} model provides the possibility to specifically deplete CD64^{+} MPs but not cDC1 and cDC2. The advantage of this model is that it can deplete CD64^{+} MPs with high specificity and efficiency. In steady state, one dose of DT injection in this model can provide a restricted CD64^{+} MPs depletion without affecting other populations at least for 3 days, so in this window Clec9a^{cre}CD64^{iDTR} model provides a powerful tool for studying AKI.

Comparing with other MPs depletion model such as CD11c-DTR mice, Clec9a^{cre}CD64^{iDTR} mice not only provides the depletion efficiency and specificity, but also do not induce neutrophilia. It is reported after CD11c^{+} cells depletion the mice are induced of neutrophilia, for studying DCs´ function in kidney this is not a good sign since the phenotype cannot be exclusively attributed to the loss of DCs or the neutrophilia. In Clec9a^{cre}CD64^{iDTR} mice we did not see neutrophilia after CD64^{+} MPs depletion.

Although we did not see increased neutrophilia after CD64^{+} MPs depletion, we saw a slight increase of MHCII^{+}Ly6C^{+} cells infiltrated into the kidney. It is possible these monocytes may fill the newly opened niche that occupied by CD64^{+} MPs before depletion. Similar thing also happened when Kupffer cells are depleted in the liver, the monocytes are infiltrated into the niche to replenish (92-94). Regarding MHCII^{+}Ly6C^{+} cells´ function in kidney during depletion, we are not sure about it, but considering their circulating monocyte like phenotype, they may infiltrate into the kidney and then differentiate into macrophages to uptake cell debris from apoptotic CD64^{+} MPs.

After we depleted CD64^{+} MPs and then induced AKI by cisplatin injection, we found 2 days later cDC1 and cDC2 reduced in cell number. However, this is unlikely due unspecific depletion of cDCs but rather because of disease triggered cell loss. This is supported by the fact that when treating Clec9a^{cre}Rosa^{YFP} mice with cisplatin we found cDC1 and cDC2 both decreased significantly in kidneys compared to NaCl injected mice, meaning the loss of cDC1 and cDC2 in Clec9a^{cre}CD64^{iDTR} mice is not due to CD64^{+} MPs depletion but cisplatin induced disease itself.

Serum urea and creatinine are 2 parameters that are widely used for evaluating kidney function. We found CD64^{+} MPs depletion leads to severer kidney damage by increased

serum urea, however, creatinine does not change significantly. One possible reason is that serum urea is more sensitive than creatinine to reflect kidney damage compare with creatinine, considering the check time point is 2 days after cisplatin treatment, creatinine might not be synthesized sufficiently to meet the detection minimum threshold.

KIM-1 is a kidney injury marker to assess the severity of AKI, interestingly, we found KIM-1 is decreased after $CD64^+$ MPs depletion instead of increase. The paradox may due to KIM-1 also serves as inhibitor for inflammatory cytokines produced by epithelial cells. Therefore, it may suppress inflammation in cisplatin induced AKI hence ameliorates injury severity at the presence of $CD64^+$ MPs, however, the depletion of $CD64^+$ MPs may reduce KIM-1 expression in total so that inflammation increased.

2. CD64+ MPs have an important role in maintaining normal kidney function in steady state and inflammation only 5 days after surgery

In order to investigate $CD64^+$ MPs role in IRI induced AKI, we firstly depleted this population and then induced the injury. We found that $CD64^+$ MPs have protective role 5 days after IRI surgery, and we also found $CD64^+$ MPs depletion without IRI surgery leads to decreased GFR on Day 5, indicating this population not only protects kidney function in inflammation but also maintains kidney function in steady state 5 days after surgery.

We did not see significantly reduced GFR after $CD64^+$ MPs depletion in short term inflammation (1 day after surgery), neither see significantly reduced GFR in $CD64^+$ MP-depleted mice 1 day after Sham surgery. It could be possible that IRI surgery induced function loss on Day 1 is too robust that masks $CD64^+$ MPs' protective effect, and the reason we can see GFR reduction on Day 5 is due to the ebb of surgery effect that exposes out $CD64^+$ MPs function. Same situation could also happen in mice with sham surgery on Day 1 since sham operation can also induce robust inflammation which may cover up $CD64^+$ MPs' effect on protecting kidney function.

One thing interesting in the $CD64^+$ MPs depleted mice 5 days after sham surgery showed that $CD64^+$ MPs kept disappeared only in contralateral kidneys but not the sham operated

kidneys, meanwhile B cells and T cells are also reduced in contralateral kidneys. It indicates the tight connection between $CD64^+$ MPs with B cells and T cells that they may not survive without $CD64^+$ MPs. It could be analogically similar with the situation in brain, neurons are the major cell in maintaining brain functions, and the rest of the populations such as astrocytes are important to support neuronal functions (95, 96). For $CD64^+$ MPs, considering their large quantity, they may serve as supporting cells for B cells and T cells mediated adaptive immune responses.

It is interesting that the loss of T cells after $CD64^+$ MPs depletion 5 days after Sham surgery is not due to reduced cDC1/cDC2 cells priming, because as professional APC, cDC1/cDC2 should be the major populations to prime naïve T cells during inflammation. When we removed cDC1 and induced IRI injury, we found T cells number did not change, it may indicate in the kidney the population to activate T cells is not cDCs but $CD64^+$ MPs in both steady state and inflammation state. It is reported $CD64^+$ MPs have strong in vitro OT-II cell priming ability, it indicates renal T cell activation in inflammation may act via $CD64^+$ MPs instead of cDCs (74).

Taken together, kidney function changes along with time post sham/IRI surgery, and $CD64^+$ MPs' protective role shows up at later time after surgery. We believe $Clec9a^{cre}CD64^{iDTR}$ mice are useful tool to study how $CD64^+$ MPs maintain renal homeostasis in both steady state and inflammation in recovery phase.

3. Outlook

During studying $CD64^+$ MPs function in IRI induced AKI, we performed unilateral IRI surgery to the mice and left the contralateral kidney untouched, in this case the GFR value actually reflects the contralateral kidney function but not the kidneys that underwent IRI surgery, since the contralateral kidney is compensating the loss of function of IRI operated kidney. In order to precisely evaluate $CD64^+$ MPs function in IRI, in the future we may use bilateral IRI model or unilateral nephrectomy (UNx) IRI model to exclude the compensation from contralateral kidney.

We saw changes of kidney function from acute injury phase to recovery phase, however we only measured Day 1 and Day 5 as beginning and ending, to precisely determine the change day by day so that we can get more information how depletion influence the injury.

Since we saw T cells and B cells decreased after $CD64^+$ MPs depletion in sham operated mice along with decreased GFR, we think these 2 populations may directly mediated the injury severity of IRI. In the future, we may use T cell or B cell depletion model to see if kidney function decreases similar as after $CD64^+$ MPs depletion 5 days after sham surgery.

We believe in kidney $CD64^+$ MPs are the major APC to activate T cell proliferation instead of cDCs, since kidney has high osmolarity that $CD64^+$ MPs may be more efficient than renal cDCs to prime T cells. It is reported $CD64^+$ MPs´ T cell activation ability in vitro is slightly lower than splenic cDC2, however if we can compare renal cDC2 with $CD64^+$ MPs to activate T cells we may find out which population has stronger T cell activation ability.

We found $CD64^+$ MPs stimulated by histone in vitro upregulated cytokines, indicating these cytokines may mediate the severity of IRI. To confirm these cytokines' function, we may use neutralizing antibodies to block these cytokines and then induced the IRI injury to see if the antibody treatment mice have severer kidney injury.

References

1. Guilliams M, Ginhoux F, Jakubzick C, Naik SH, Onai N, Schraml BU, et al. Dendritic cells, monocytes and macrophages: a unified nomenclature based on ontogeny. Nat Rev Immunol. 2014;14(8):571-8.

2. Collin M, Bigley V. Human dendritic cell subsets: an update. Immunology. 2018;154(1):3-20.

3. Sichien D, Lambrecht BN, Guilliams M, Scott CL. Development of conventional dendritic cells: from common bone marrow progenitors to multiple subsets in peripheral tissues. Mucosal Immunology. 2017;10(4):831-44.

4. Onai N, Obata-Onai A, Schmid MA, Ohteki T, Jarrossay D, Manz MG. Identification of clonogenic common Flt3+M-CSFR+ plasmacytoid and conventional dendritic cell progenitors in mouse bone marrow. Nature Immunology. 2007;8(11):1207-16.

5. Chistiakov DA, Orekhov AN, Sobenin IA, Bobryshev YV. Plasmacytoid dendritic cells: development, functions, and role in atherosclerotic inflammation. Front Physiol. 2014;5:279-.

6. Tai Y, Wang Q, Korner H, Zhang L, Wei W. Molecular Mechanisms of T Cells Activation by Dendritic Cells in Autoimmune Diseases. Front Pharmacol. 2018;9:642-.

7. Dempsey LA. cDC1 cross-priming. Nature Immunology. 2019;20(1):1-.

8. Hilligan KL, Ronchese F. Antigen presentation by dendritic cells and their instruction of CD4+ T helper cell responses. Cell Mol Immunol. 2020;17(6):587-99.

9. Liu Z, Roche PA. Macropinocytosis in phagocytes: regulation of MHC class-II-restricted antigen presentation in dendritic cells. Front Physiol. 2015;6(1).

10. Vatner RE, Janssen EM. STING, DCs and the link between innate and adaptive tumor immunity. Mol Immunol. 2019;110:13-23.

11. Schraml, B., U., van?Blijswijk, J., Zelenay, et al. Genetic Tracing via DNGR-1 Expression History Defines Dendritic Cells as a Hematopoietic Lineage. Cell Cambridge Ma. 2013.

12. Ferris ST, Durai V, Wu R, Theisen DJ, Ward JP, Bern MD, et al. cDC1 prime and are licensed by CD4(+) T cells to induce anti-tumour immunity. Nature. 2020;584(7822):624-9.

13. Musumeci A, Lutz K, Winheim E, Krug AB. What Makes a pDC: Recent Advances in Understanding Plasmacytoid DC Development and Heterogeneity. Frontiers in Immunology. 2019;10(1222).

14. Vremec D, O'Keeffe M, Hochrein H, Fuchsberger M, Caminschi I, Lahoud M, et al. Production of interferons by dendritic cells, plasmacytoid cells, natural killer cells, and interferon-producing killer dendritic cells. Blood. 2006;109(3):1165-73.

15. Dinarello CA. Overview of the IL-1 family in innate inflammation and acquired immunity. Immunol Rev. 2018;281(1):8-27.

16. Ren K, Torres R. Role of interleukin-1beta during pain and inflammation. Brain Res Rev. 2009;60(1):57-64.

17. Kaneko N, Kurata M, Yamamoto T, Morikawa S, Masumoto J. The role of interleukin-1 in general pathology. Inflammation and Regeneration. 2019;39(1):12.

18. Wan C-K, Li P, Spolski R, Oh J, Andraski AB, Du N, et al. IL-21-mediated non-canonical pathway for IL-1β production in conventional dendritic cells. Nature Communications. 2015;6(1):7988.

19. Wesa AK, Anne G. IL-1β induces dendritic cells to produce IL-12. International Immunology. 2001(8):1053.

20. Abdi K, Singh NJ, Matzinger P. Lipopolysaccharide-activated dendritic cells: "exhausted" or alert and waiting? J Immunol. 2012;188(12):5981-9.

21. Wilkinson AN, Chang K, Kuns RD, Henden AS, Minnie SA, Ensbey KS, et al. IL-6 dysregulation originates in dendritic cells and mediates graft-versus-host disease via classical signaling. Blood. 2019;134(23):2092-106.

22. Gubernatorova EO, Gorshkova EA, Namakanova OA, Zvartsev RV, Hidalgo J, Drutskaya MS, et al. Non-redundant Functions of IL-6 Produced by Macrophages and Dendritic Cells in Allergic Airway Inflammation. Frontiers in Immunology. 2018;9(2718).

23. Dodge IL, Carr MW, Cernadas M, Brenner MB. IL-6 Production by Pulmonary Dendritic Cells Impedes Th1 Immune Responses. The Journal of Immunology. 2003;170(9):4457-64.

24. Heink S, Yogev N, Garbers C, Herwerth M, Aly L, Gasperi C, et al. Trans-presentation of IL-6 by dendritic cells is required for the priming of pathogenic T(H)17 cells. Nature immunology. 2017;18(1):74-85.

25. Akbari O, DeKruyff RH, Umetsu DT. Pulmonary dendritic cells producing IL-10 mediate tolerance induced by respiratory exposure to antigen. Nature Immunology. 2001;2(8):725-31.

26. Corinti S, Albanesi C, la Sala A, Pastore S, Girolomoni G. Regulatory Activity of Autocrine IL-10 on Dendritic Cell Functions. The Journal of Immunology. 2001;166(7):4312-8.

27. Suen J-L, Chang Y, Shiu Y-S, Hsu C-Y, Sharma P, Chiu C-C, et al. IL-10 from plasmacytoid dendritic cells promotes angiogenesis in the early stage of endometriosis. The Journal of pathology. 2019;249(4):485-97.

28. Schülke S. Induction of Interleukin-10 Producing Dendritic Cells As a Tool to Suppress Allergen-Specific T Helper 2 Responses. Frontiers in Immunology. 2018;9(455).

29. Zhou F, Ciric B, Li H, Yan Y, Li K, Cullimore M, et al. IL-10 deficiency blocks the ability of LPS to regulate expression of tolerance-related molecules on dendritic cells. European journal of immunology. 2012;42(6):1449-58.

30. Wu Y, Hirschi KK. Tissue-Resident Macrophage Development and Function. Front Cell Dev Biol. 2021;8:617879-.

31. Bian Z, Gong Y, Huang T, Lee CZW, Bian L, Bai Z, et al. Deciphering human macrophage development at single-cell resolution. Nature. 2020;582(7813):571-6.

32. Hoeffel G, Ginhoux F. Ontogeny of Tissue-Resident Macrophages. Frontiers in Immunology. 2015;6(486).

33. McGrath KE, Frame JM, Palis J. Early hematopoiesis and macrophage development. Semin Immunol. 2015;27(6):379-87.

34. Guilliams M, Bruhns P, Saeys Y, Hammad H, Lambrecht BN. The function of Fcγ receptors in dendritic cells and macrophages. Nature Reviews Immunology. 2014;14(2):94-108.

35. Huynh L, Wang L, Shi C, Park-Min K-H, Ivashkiv LB. ITAM-coupled receptors inhibit IFNAR signaling and alter macrophage responses to TLR4 and Listeria monocytogenes. J Immunol. 2012;188(7):3447-57.

36. Lewis A, Elks PM. Hypoxia Induces Macrophage tnfa Expression via Cyclooxygenase and Prostaglandin E2 in vivo. Frontiers in Immunology. 2019;10(2321).

37. Westra J, Doornbos-van der Meer B, de Boer P, van Leeuwen MA, van Rijswijk MH, Limburg PC. Strong inhibition of TNF-alpha production and inhibition of IL-8 and COX-2 mRNA expression in monocyte-derived macrophages by RWJ 67657, a p38 mitogen-activated protein kinase (MAPK) inhibitor. Arthritis Res Ther. 2004;6(4):R384-R92.

38. Eliopoulos AG, Dumitru CD, Wang C-C, Cho J, Tsichlis PN. Induction of COX-2 by LPS in macrophages is regulated by Tpl2-dependent CREB activation signals. The EMBO Journal. 2002;21(18):4831-40.

39. Giulian D, Baker TJ, Shih LC, Lachman LB. Interleukin 1 of the central nervous system is produced by ameboid microglia. J Exp Med. 1986;164(2):594-604.

40. Arango Duque G, Descoteaux A. Macrophage cytokines: involvement in immunity and infectious diseases. Frontiers in immunology. 2014;5:491-.

41. Drysdale BE, Zacharchuk CM, Shin HS. Mechanism of macrophage-mediated cytotoxicity: production of a soluble cytotoxic factor. The Journal of Immunology. 1983;131(5):2362-7.

42. Misharin AV, Morales-Nebreda L, Mutlu GM, Budinger GRS, Perlman H. Flow Cytometric Analysis of Macrophages and Dendritic Cell Subsets in the Mouse Lung. American Journal of Respiratory Cell and Molecular Biology. 2013;49(4):503-10.

43. Yu Y-RA, O'Koren EG, Hotten DF, Kan MJ, Kopin D, Nelson ER, et al. A Protocol for the Comprehensive Flow Cytometric Analysis of Immune Cells in Normal and Inflamed Murine Non-Lymphoid Tissues. PLoS One. 2016;11(3):e0150606-e.

44. Puranik AS, Leaf IA, Jensen MA, Hedayat AF, Saad A, Kim K-W, et al. Kidney-resident macrophages promote a proangiogenic environment in the normal and chronically ischemic mouse kidney. Scientific Reports. 2018;8(1):13948.

45. Malissen B, Tamoutounour S, Henri S. The origins and functions of dendritic cells and macrophages in the skin. Nature Reviews Immunology. 2014;14(6):417-28.

46. Gottschalk C, Kurts C. The Debate about Dendritic Cells and Macrophages in the Kidney. Frontiers in Immunology. 2015;6(435).

47. Weisheit CK, Engel DR, Kurts C. Dendritic Cells and Macrophages: Sentinels in the Kidney. Clinical Journal of the American Society of Nephrology. 2015;10(10):1841-51.

48. Rogers NM, Ferenbach DA, Isenberg JS, Thomson AW, Hughes J. Dendritic cells and macrophages in the kidney: a spectrum of good and evil. Nature Reviews Nephrology. 2014;10(11):625-43.

49. Salei N, Rambichler S, Salvermoser J, Papaioannou NE, Schuchert R, Pakalniškytė D, et al. The Kidney Contains Ontogenetically Distinct Dendritic Cell and Macrophage Subtypes throughout Development That Differ in Their Inflammatory Properties. Journal of the American Society of Nephrology : JASN. 2020;31(2):257-78.

50. Lever JM, Hull TD, Boddu R, Pepin ME, Black LM, Adedoyin OO, et al. Resident macrophages reprogram toward a developmental state after acute kidney injury. JCI insight. 2019;4(2):e125503.

51. Chen T, Cao Q, Wang R, Zheng G, Azmi F, Wang J, et al. Conventional Type 1 Dendritic Cells (cDC1) in Human Kidney Diseases: Clinico-Pathological Correlations. Frontiers in immunology. 2021;12:635212-.

52. Li N, Steiger S, Fei L, Li C, Shi C, Salei N, et al. IRF8-Dependent Type I Conventional Dendritic Cells (cDC1s) Control Post-Ischemic Inflammation and Mildly

Protect Against Post-Ischemic Acute Kidney Injury and Disease. Frontiers in immunology. 2021;12:685559-.

53. Price JD, Tarbell KV. The Role of Dendritic Cell Subsets and Innate Immunity in the Pathogenesis of Type 1 Diabetes and Other Autoimmune Diseases. Frontiers in immunology. 2015;6:288-.

54. Brown CC, Gudjonson H, Pritykin Y, Deep D, Lavallée V-P, Mendoza A, et al. Transcriptional Basis of Mouse and Human Dendritic Cell Heterogeneity. Cell. 2019;179(4):846-63.e24.

55. Sathaliyawala T, O'Gorman WE, Greter M, Bogunovic M, Konjufca V, Hou ZE, et al. Mammalian target of rapamycin controls dendritic cell development downstream of Flt3 ligand signaling. Immunity. 2010;33(4):597-606.

56. Lean JM, Fuller K, Chambers TJ. FLT3 ligand can substitute for macrophage colony-stimulating factor in support of osteoclast differentiation and function. Blood. 2001;98(9):2707-13.

57. Karsunky H, Merad M, Cozzio A, Weissman IL, Manz MG. Flt3 ligand regulates dendritic cell development from Flt3+ lymphoid and myeloid-committed progenitors to Flt3+ dendritic cells in vivo. J Exp Med. 2003;198(2):305-13.

58. Servet-Delprat C, Arnaud S, Jurdic P, Nataf S, Grasset M-F, Soulas C, et al. Flt3+ macrophage precursors commit sequentially to osteoclasts, dendritic cells and microglia. BMC Immunology. 2002;3(1):15.

59. Brasel K, De Smedt T, Smith JL, Maliszewski CR. Generation of murine dendritic cells from flt3-ligand–supplemented bone marrow cultures. Blood. 2000;96(9):3029-39.

60. Liu Z, Gu Y, Chakarov S, Bleriot C, Ginhoux F. Fate Mapping via Ms4a3-Expression History Traces Monocyte-Derived Cells. Cell. 2019;178(6):1509-25.e19.

61. Yang Q, Wang Y, Pei G, Deng X, Jiang H, Wu J, et al. Bone marrow-derived Ly6C− macrophages promote ischemia-induced chronic kidney disease. Cell Death & Disease. 2019;10(4):291.

62. Atala A. Re: Renal Sodium Gradient Orchestrates a Dynamic Antibacterial Defense Zone. Journal of Urology. 2018;199(5):1116-.

63. Stamatiades EG, Tremblay M-E, Bohm M, Crozet L, Bisht K, Kao D, et al. Immune Monitoring of Trans-endothelial Transport by Kidney-Resident Macrophages. Cell. 2016;166(4):991-1003.

64. Salei N, Rambichler S, Salvermoser J, Papaioannou NE, Schuchert R, Pakalniškytė D, et al. The Kidney Contains Ontogenetically Distinct Dendritic Cell and Macrophage Subtypes throughout Development That Differ in Their Inflammatory Properties. Journal of the American Society of Nephrology. 2020;31(2):257-78.

65. Lu L, Faubel S, He Z, Andres Hernando A, Jani A, Kedl R, et al. Depletion of macrophages and dendritic cells in ischemic acute kidney injury. American journal of nephrology. 2012;35(2):181-90.

66. Tadagavadi RK, Gao G, Wang WW, Gonzalez MR, Reeves WB. Dendritic Cell Protection from Cisplatin Nephrotoxicity Is Independent of Neutrophils. Toxins (Basel). 2015;7(8):3245-56.

67. Malek M, Nematbakhsh M. Renal ischemia/reperfusion injury; from pathophysiology to treatment. Journal of renal injury prevention. 2015;4(2):20-7.

68. Nieuwenhuijs-Moeke GJ, Pischke SE, Berger SP, Sanders JSF, Pol RA, Struys MMRF, et al. Ischemia and Reperfusion Injury in Kidney Transplantation: Relevant Mechanisms in Injury and Repair. Journal of clinical medicine. 2020;9(1):253.

69. Skrypnyk NI, Harris RC, de Caestecker MP. Ischemia-reperfusion model of acute kidney injury and post injury fibrosis in mice. J Vis Exp. 2013(78):50495.

70. Ozkok A, Edelstein CL. Pathophysiology of cisplatin-induced acute kidney injury. Biomed Res Int. 2014;2014:967826-.

71. McSweeney KR, Gadanec LK, Qaradakhi T, Ali BA, Zulli A, Apostolopoulos V. Mechanisms of Cisplatin-Induced Acute Kidney Injury: Pathological Mechanisms, Pharmacological Interventions, and Genetic Mitigations. Cancers (Basel). 2021;13(7):1572.

72. Li L, Okusa MD. Macrophages, dendritic cells, and kidney ischemia-reperfusion injury. Semin Nephrol. 2010;30(3):268-77.

73. Ferenbach DA, Sheldrake TA, Dhaliwal K, Kipari T, Marson LP, Kluth DC, et al. Macrophage/monocyte depletion by clodronate, but not diphtheria toxin, improves renal ischemia/reperfusion injury in mice. Kidney International. 2012;82(8):928-33.

74. Kitamoto K, Machida Y, Uchida J, Izumi Y, Miura K. Effects of liposome clodronate on renal leukocyte populations and renal fibrosis in murine obstructive nephropathy. Journal of Pharmacological Sciences. 2009;111(3):285.

75. Schraml B, Van?Blijswijk J, Zelenay S, Whitney P, Filby A, Acton S, et al. Genetic tracing via DNGR-1 expression history defines dendritic cells as a hematopoietic lineage. Cell. 2013;154(4):843-58.

76. Salei N, Ji X, Pakalniškytė D, Kuentzel V, Rambichler S, Li N, et al. Selective depletion of a CD64-expressing phagocyte subset mediates protection against toxic kidney injury and failure. Proc Natl Acad Sci U S A. 2021;118(39):e2022311118.

77. Srinivas, Shankar, Watanabe, Tomoko, Lin CS, William, et al. Cre reporter strains produced by targeted insertion of EYFP and ECFP into the ROSA26 locus. BMC Developmental Biology. 2001.

78. Buch T, Heppner FL, Tertilt C, Heinen TJAJ, Kremer M, Wunderlich FT, et al. A Cre-inducible diphtheria toxin receptor mediates cell lineage ablation after toxin administration. Nature Methods. 2005;2(6):419.

79. Klein U, Ca Sola S, Ca Ttoretti G, Shen Q, Lia M, Mo T, et al. Transcription factor IRF4 controls plasma cell differentiation and class-switch recombination. Nature Immunology. 2006;7(7):773-82.

80. Yamazaki C, Sugiyama M, Ohta T, Hemmi H, Hamada E, Sasaki I, et al. Critical Roles of a Dendritic Cell Subset Expressing a Chemokine Receptor, XCR1. Journal of Immunology. 2013;190(12):6071-82.

81. Schlitzer A, McGovern N, Teo P, Zelante T, Atarashi K, Low D, et al. IRF4 transcription factor-dependent CD11b+ dendritic cells in human and mouse control mucosal IL-17 cytokine responses. Immunity. 2013;38(5):970-83.

82. Persson EK, Uronen-Hansson H, Semmrich M, Rivollier A, Hägerbrand K, Marsal J, et al. IRF4 transcription-factor-dependent CD103(+)CD11b(+) dendritic cells drive mucosal T helper 17 cell differentiation. Immunity. 2013;38(5):958-69.

83. Yang L, Brooks CR, Xiao S, Sabbisetti V, Bonventre JV. KIM-1–mediated phagocytosis reduces acute injury to the kidney. Journal of Clinical Investigation. 2015;125(4).

84. Tittel AP, Heuser C, Ohliger C, Llanto C, Yona S, Hämmerling GJ, et al. Functionally relevant neutrophilia in CD11c diphtheria toxin receptor transgenic mice. Nat Methods. 2012;9(4):385-90.

85. Kinsey GR, Okusa MD. Expanding role of T cells in acute kidney injury. Curr Opin Nephrol Hypertens. 2014;23(1):9-16.

86. Ko GJ, Jang HR, Huang Y, Womer KL, Liu M, Higbee E, et al. Blocking Fas ligand on leukocytes attenuates kidney ischemia-reperfusion injury. Journal of the American Society of Nephrology : JASN. 2011;22(4):732-42.

87. Akcay A, Nguyen Q, He Z, Turkmen K, Won Lee D, Hernando AA, et al. IL-33 exacerbates acute kidney injury. Journal of the American Society of Nephrology : JASN. 2011;22(11):2057-67.

88. Tittel AP, Heuser C, Ohliger C, Llanto C, Yona S, H?mmerling GJ, et al. Functionally relevant neutrophilia in CD11c diphtheria toxin receptor transgenic mice. Nature Methods. 2012;9(4):385-90.

89. Kielar, M. L. Maladaptive Role of IL-6 in Ischemic Acute Renal Failure. Journal of the American Society of Nephrology. 2005;16(11):3315-25.

90. Liang H, Xu F, Zhang T, Huang J, Huang Q. Inhibition of IL-18 reduces renal fibrosis after ischemia-reperfusion. Biomedicine & pharmacotherapy = Biomedecine & pharmacotherapie. 2018;106:879-89.

91. Huang L, Zhang R, Wu J, Chen J, Grosjean F, Satlin LH, et al. Increased susceptibility to acute kidney injury due to endoplasmic reticulum stress in mice lacking tumor necrosis factor-α and its receptor 1. Kidney International. 2011;79(6):613-23.

92. Allam R, Scherbaum CR, Darisipudi MN, Mulay SR, Hägele H, Lichtnekert J, et al. Histones from dying renal cells aggravate kidney injury via TLR2 and TLR4. Journal of the American Society of Nephrology : JASN. 2012;23(8):1375-88.

93. Roohani S, Tacke F. Liver Injury and the Macrophage Issue: Molecular and Mechanistic Facts and Their Clinical Relevance. Int J Mol Sci. 2021;22(14).

94. Wen Y, Lambrecht J, Ju C, Tacke F. Hepatic macrophages in liver homeostasis and diseases-diversity, plasticity and therapeutic opportunities. Cell Mol Immunol. 2021;18(1):45-56.

95. Helk E, Bernin H, Ernst T, Ittrich H, Jacobs T, Heeren J, et al. TNFα-mediated liver destruction by Kupffer cells and Ly6Chi monocytes during Entamoeba histolytica infection. PLoS Pathog. 2013;9(1):e1003096.

96. Kim Y, Park J, Choi YK. The Role of Astrocytes in the Central Nervous System Focused on BK Channel and Heme Oxygenase Metabolites: A Review. Antioxidants (Basel). 2019;8(5).

97. Perez-Catalan NA, Doe CQ, Ackerman SD. The role of astrocyte-mediated plasticity in neural circuit development and function. Neural Development. 2021;16(1):1.

Acknowledgements

Firstly I want to thank my supervisor Prof. Dr. Barbara Schraml offers me the chance to persue my Ph.D in her lab. In the past 3 years, I gained a lot of suppport from her and her supervison makes my project a successful one.

I also want to thank my TAC members, Prof. Dr. med. Hans-Joachim Anders and Prof. Dr. med. Markus Sperandio for giving me valuable advices to my project, which makes the project scientifically invincible.

I would also thank Dr. Julia Lichtnekert, Ms. Na Li and Mr. Chenyu Li from AG Anders to organize the surgery for my project, my project went smoothly with their help.

Special thanks to my lab mates from AG Schraml, Dr. Natallia Salei, Dr. Stephan Rambichler, Ms. Vanessa Küntzel offered constructive work to my project, Ms. Hamsa Narasimhan, Mr. Ramin Shakiba, Mr. Dogus Altunöz, Mr. Kaushikk Ravi gave wonderful advices to my work.

I also thank all members from SFB914 to support my work in the past 3 years, my special thank to Dr. Verena Kochan for organizing and coordinating my Ph.D training.

Finally I would thank my family for supporting me doing Ph.D in Germany, without their help I would not have this wonderful experience, and I can always get helpful advices from them whenever I need.

Appendix

Publicaitons related to this work

Salei N, Ji X, Pakalniškytė D, Kuentzel V, Rambichler S, Li N, et al. Selective depletion of a CD64-expressing phagocyte subset mediates protection against toxic kidney injury and failure. Proc Natl Acad Sci U S A. 2021;118(39):e2022311118.

LMU LUDWIG-MAXIMILIANS-UNIVERSITÄT MÜNCHEN

Dean's Office
Medical Faculty

MMRS

Affidavit

Ji, Xingqi

Surname, first name

Street

Zip code, town

Country

I hereby declare, that the submitted thesis entitled

Renal CD64+ MPs protect kidney in both cisplatin and ischemia reperfusion induced acute kidney injury

is my own work. I have only used the sources indicated and have not made unauthorised use of services of a third party. Where the work of others has been quoted or reproduced, the source is always given.

I further declare that the dissertation presented here has not been submitted in the same or similar form to any other institution for the purpose of obtaining an academic degree.

Chapel Hill, 17.06.2024

Place, date

Xingqi Ji

Signature doctoral candidate

LMU LUDWIG-MAXIMILIANS-UNIVERSITÄT MÜNCHEN

Dean's Office
Medical Faculty

MMRS

Confirmation of congruency between printed and electronic version of the doctoral thesis

Ji, Xingqi

Surname, first name

Street

Zip code, town

Country

I hereby declare that the electronic version of the submitted thesis, entitled

Renal CD64+ MPs protect kidney in both cisplatin and ischemia reperfusion induced acute kidney injury

is congruent with the printed version both in content and format.

Chapel Hill, 17.06.2024

Place, date

Xingqi Ji

Signature doctoral candidate